NPS-ME-94-007

NAVAL POSTGRADUATE SCHOOL
MONTEREY, CALIFORNIA

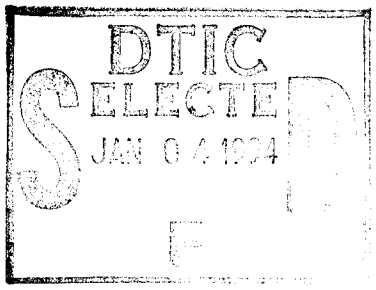

RESPONSE OF DUAL-LAYERED STRUCTURES SUBJECTED TO SHOCK PRESSURE WAVE

by

LT T.P. Brasek, USN
Professor Y.W. Kwon, Co-Investigator
Professor Y.S. Shin, Principal Investigator

October 1, 1994 - December 31, 1994

Approved for public release; distribution is unlimited.

Prepared for: Defense Nuclear Agency
Alexandria, VA 20311

Naval Postgraduate School
Monterey, CA 93940

Naval Postgraduate School
Monterey, California

Rear Admiral T.A. Mercer
Superindendent

H. Shull
Provost

This report was prepared for and fully funded by both the Defense Nuclear Agency, Alexandria, VA 20311 and the Naval Postgraduate School, Monterey, CA 93943.

This report was prepared by:

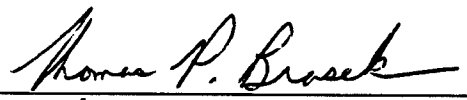

T.P. Brasek
LT, USN

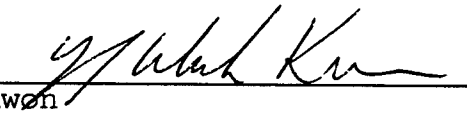

Y.W. Kwon
Associate Professor of Mechanical Engineering

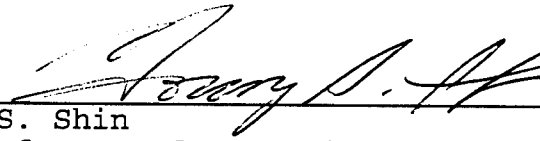

Y.S. Shin
Professor of Mechanical Engineering

Reviewed by:

M.D. Kelleher
Chairman
Dept. of Mechanical Eng.

Released by:

P.J. Marto
Dean of Research

REPORT DOCUMENTATION PAGE

Form Approved OMB No. 0704-0188

1. AGENCY USE ONLY *(Leave blank)*	2. REPORT DATE December 31, 1994	3. REPORT TYPE AND DATES COVERED Progress Report from October 1, 1994 to December 31, 1994

4. TITLE AND SUBTITLE Response of Dual-Layered Structures Subjected to Shock Pressure Wave

5. FUNDING NUMBERS MIPR No. 94-573

6. AUTHOR(S) T.P. Brasek, Y.W. Kwon, and Y.S. Shin

7. PERFORMING ORGANIZATION NAME(S) AND ADDRESS(ES)
Naval Postgraduate School
Monterey CA 93943-5000

8. PERFORMING ORGANIZATION REPORT NUMBER NPS-ME-94-007

9. SPONSORING/MONITORING AGENCY NAME(S) AND ADDRESS(ES)
Defense Nuclear Agency Alexandria ,VA 20311

10. SPONSORING/MONITORING AGENCY REPORT NUMBER

11. SUPPLEMENTARY NOTES The views expressed in this thesis are those of the author and do not reflect the official policy or position of the Department of Defense or the U.S. Government.

12a. DISTRIBUTION/AVAILABILITY STATEMENT
Approved for public release; distribution is unlimited.

12b. DISTRIBUTION CODE

13. ABSTRACT *(maximum 200 words)*

The response of coated, metallic structures subjected to shock pressure waves is studied. The coating is either an elastic material or nearly incompressible rubber of variable stiffness separating the structure from an air or water medium. The stress, nodal velocity, and internal energy of the coated structure are compared to a system without a coating (homogeneous system) to examine the effect of various coating types and configurations on the response of the structure to shock conditions.

The results show that a mismatch of impedance, ρc_o, between the coating and structure governs the degree of energy exchange between the coating and structure at the interface. The impedance mismatch between the structure and a rubber coating at the threshold value is termed the critical difference. If the impedance mismatch exceeds the critical difference, the dynamic response will be more adverse. A softer coating generally has a smaller impedance and tends to concentrate stress wave energy in the underlying structure.

14. SUBJECT TERMS Underwater explosion, surface coatings, impedance mismatch

15. NUMBER OF PAGES 74

16. PRICE CODE

17. SECURITY CLASSIFICATION OF REPORT	18. SECURITY CLASSIFICATION OF THIS PAGE	19. SECURITY CLASSIFICATION OF ABSTRACT	20. LIMITATION OF ABSTRACT
Unclassified	Unclassified	Unclassified	UL

NSN 7540-01-280-5500

Standard Form 298 (Rev. 2-89)

ABSTRACT

The response of coated, metallic structures subjected to shock pressure waves is studied. The coating is either an elastic material or nearly incompressible rubber of variable stiffness separating the structure from an air or water medium. The stress, nodal velocity, and internal energy of the coated structures are compared to a system without a coating (homogeneous system) to examine the effect of various coating types and configurations on the response of the structure to shock conditions.

The results show that a mismatch of impedance, ρc_o, between the coating and structure governs the degree of energy exchange between the coating and structure at the interface. An elastic coating with a smaller impedance induces a higher stress in the underlying structure. The impedance mismatch between the structure and a rubber coating at the threshold value is termed the critical difference. If the impedance mismatch exceeds the critical difference, the dynamic response will be more adverse. A softer coating generally has a smaller impedance and tends to concentrate stress wave energy in the underlying structure.

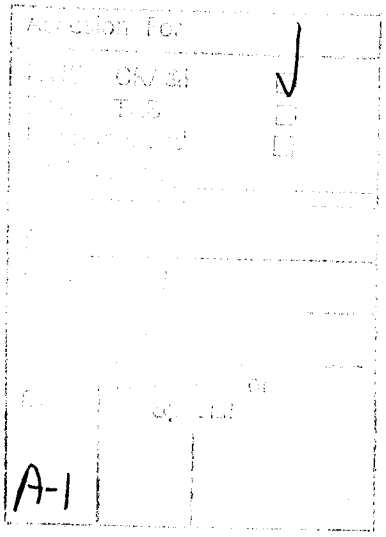

TABLE OF CONTENTS

LIST OF FIGURES

I. INTRODUCTION

Research at the Naval Postgraduate School continues in an effort to understand the dynamic response of coated structures subjected to shock waves. Past work focused on the comparison of numerical modeling to physical testing in an attempt to carry out further research more cost effectively. Cylindrical models in an underwater environment subjected to both near and far field explosions have been tested with great success. Nelson, Shin, and Kwon [Ref. 1], Fox, Kwon, and Shin [Ref. 2] and Chisum [Ref. 3] have demonstrated that the coupled computer code of the finite element method and the boundary element method closely approximate simple experimental analyses. Hence this research asserts that limited parametric studies can be conducted without needing to construct and test physical models.

Kwon, Bergersen, and Shin [Ref. 4] studied the effects of surface coatings on metal cylinders in an underwater explosive environment. Under certain impact conditions, surface coatings appear to concentrate shock energy within the structure for longer time periods. This energy concentration manifests itself in higher stress and strain magnitudes in the metal cylinder. This is the result of trapping the shock wave energy and preventing its release into the surrounding water medium.

The amount of energy retained by the cylinder is greatly affected by both the thickness and shear modulus of the coating. In general, the resultant stress, strain, and deformation decrease with an increase in coating thickness and shear modulus. Both these parameters are used to categorize the stiffness of a material, which most likely determines the degree of energy transfer between a structure and a medium. Therefore, a threshold value for coating stiffness may be determined for a particular application. Above this theoretical value, a favorable dynamic response of a coated cylinder to an underwater explosion will occur; below this

value, an adverse dynamic response results. An adverse response may entail increased strains and internal energy causing plastic deformation and failure of the structure.

Dissipation of energy into the surrounding medium is a critical factor to a structure's behavior in response to an explosion. The analysis of shock wave propagation and its effect on deformation is difficult due to the complexity of the interaction between the medium, coating, and structure.

The United States Navy has been experimenting with submarine coatings for decades. Hull coatings have been predominantly strategic in nature. For example, the rubber anechoic coating has been used as an anti-submarine warfare (ASW) tool to reduce acoustic energy reflected by the hull.

Despite the advantage provided in ASW, anechoic coatings may contribute to the adverse effects of a close-range underwater explosion. Previous studies have shown that coated cylinders have sustained greater shock damage than uncoated cylinders under identical testing conditions. The coating has prevented shock wave energy release to the surrounding water medium. This energy contributes to the plastic deformation of the metal. When applied to a submarine, such a response has disastrous results for shock blast survivability of the vessel's crew and equipment.

In order to develop a coating with both ASW advantages and shock wave survivability, the effects of the coating on the structure need to be studied in greater detail. The first step involves examining the response of a simple system to a shock front to gain a thorough understanding of the medium-coating-structure interaction. Such research will provide insight into the physics leading to the deformation and ultimate failure of the structure. A parametric, numerical study is performed on one-dimensional and two-dimensional coated aluminum structures to examine the interaction of the coating-structure-medium and stress wave physics.

II. NUMERICAL ANALYSIS

In order to study the effects of shock waves on coated structures, a finite element model is developed. The premise of this study is to garner a basic understanding of a shock pulse impact and propagation through a coated structure.

The public-domain program used to develop the coated structure system is VEC/DYNA3D, an explicit finite element code [Ref. 5]. This particular code has been utilized quite extensively at the Naval Postgraduate School for evaluating the dynamic response of structures subjected to underwater explosions. VEC/DYNA3D provides a wide assortment of material types, equations of state, and loading conditions.

The pre-processor, LS-INGRID, is used to generate the actual finite element mesh [Ref. 6]. Interfacing with VEC/DYNA3D, INGRID constructs the model with respect to desired geometries, boundary conditions, planes of symmetry, material and element types, and external forces.

The VEC/DYNA3D calculations and outputs are reviewed in LS-TAURUS, an interactive post-processor [Ref. 7]. TAURUS displays the element, node, and material time history plots and other germane dynamic response characteristics.

For water-bounded systems, the finite element method provided by VEC/DYNA3D is used to model the structure and coating, but the water is modelled using a boundary element method code. Specifically, the boundary element method employed is the Underwater Shock Analysis (USA) code with the Cavitating Fluid Analyzer (CFA) upgrade designed by DeRuntz [Ref. 8]. The doubly asymptotic approximation (DAA) developed by Geers provides the interaction between the acoustic water medium and the finite element model [Ref. 9]. The DAA reduces the number of elements needed to simulate the water medium.

III. MODEL DESCRIPTION

A. MATERIAL DESCRIPTION

An aluminum structure will be subjected to a step pressure wave not potent enough to cause plastic deformation. The material properties of the type of aluminum selected, 6061-T6, are given in Table 1. The structure will be coated with either an elastic or nearly incompressible rubber material.

Table 1. 6061-T6 Aluminum Properties

Parameter	Property/Symbol	Quantity
Density	ρ	5.447 slugs/ft^3
Poisson's Ratio	υ	0.33
Young's Modulus	E	1.08 x 10^7 psi
Yield Stress	σ_y	4.0 x 10^4 psi
Speed of sound	c_o	16,389 ft/sec

The characteristics of the rubber coating is based on the Mooney-Rivlin compression model [Refs. 5,6]. This approach is suitable to the analysis of superelastic material deformation using general strain energy density. Mooney developed a new approach to study the deformation of soft material such as rubber or foam [Ref. 10]. He stated that the strain energy density function, W, is a function of the principal stretches (1 + principal extensions) of the material, η, the shear modulus, G, and a modulus expressing the asymmetry of reciprocal deformation, H. The variable H is a measure of the material's ability to store energy when compressed as opposed when it is stretched:

$$W = \frac{G}{4}\sum_{i=1}^{3}\left(\eta_i - \frac{1}{\eta_i}\right)^2 + \frac{H}{4}\sum_{i=1}^{3}\left(\eta_i^2 - \frac{1}{\eta_i^2}\right) \qquad (1)$$

In order to lend versatility to this strain energy density theory and deformation under load, Mooney defined a new parameter which he termed the coefficient of asymmetry, α:

$$\alpha = \frac{H}{G} \tag{2}$$

Values for the variables G and α were determined experimentally for tread stock rubber. Experimental data conducted with rubber undergoing up to 400% elongation and 50% compression correlated well with the analysis results. Thus the deformation of the rubber is characterized by the shear modulus and the coefficient of asymmetry.

The nearly incompressible Mooney-Rivlin rubber is implemented into VEC/DYNA3D to formulate the finite element model with the rubber coating. The code requires two input constants, A and B. These two values are determined by the rubber shear modulus and coefficient of asymmetry as follows:

$$A = \frac{G}{4}(1 + \alpha) \tag{3}$$

$$B = \frac{G}{4}(1 - \alpha) \tag{4}$$

Tread stock rubber has the properties listed in Table 2.

Table 2. Tread Stock Rubber Properties

Parameter	Property/Symbol	Quantity
Density	ρ	1.908 slugs/ft^3
Shear Modulus	G	95.8 psi
Speed of sound	c_o	100 ft/sec
Asymmetry coeff.	α	0.223

B. GEOMETRIC DESCRIPTION

1. Description of one-dimensional model

The model used for the first phase of this study is a simple, one-dimensional system consisting of a coated structure subjected to a unit step pressure wave (Figure 1a). The structure material is 6061-T6 aluminum, a widely-applied metal with excellent elastic properties; the coating is an elastic material or superelastic rubber. One end of the system interfaces with either air or water and is free to displace; the other end is fixed. The step wave impacts the free end and propagates through both the coating and the structure. This parametric study analyzes a finite element model consisting of 8-node hexahedral brick elements. The major axis is in the x-direction. The system is bounded by the xy and xz symmetry planes. The structure and coating consist of 52 solid elements apiece; the overall system is composed of 420 nodes (Figure 1b).

2. Description of two-dimensional model

The models used in the second phase of this study are uncoated and coated infinite cylinders bounded externally by water and subjected to a unit step pressure wave (Figure 2a). The cylindrical shell is 6061-T6 aluminum while the coating is either an elastic material or superelastic rubber. The model is bounded by three symmetry planes reducing the infinite cylinder to a half-model problem. The z-axis is the longitudinal direction. The coating and structure consist of 24 elements apiece for a total of 150 nodes (Figure 2b).

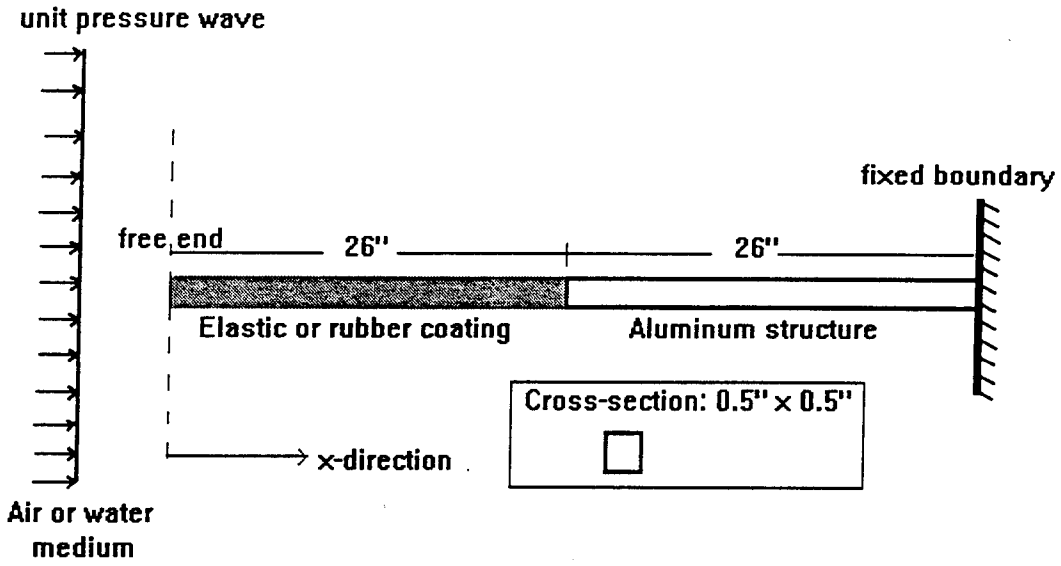

Figure 1a. One-dimensional system with symmetrical boundaries on all sides subjected to unit step pressure wave

one-dimensional system

Figure 1b. Finite element model of one-dimensional system

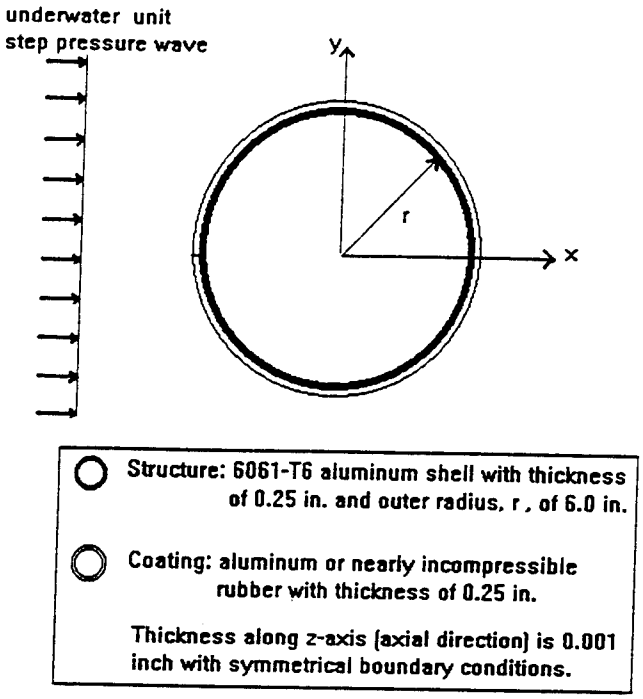

Figure 2a. Infinite cylinder subjected to unit step pressure wave

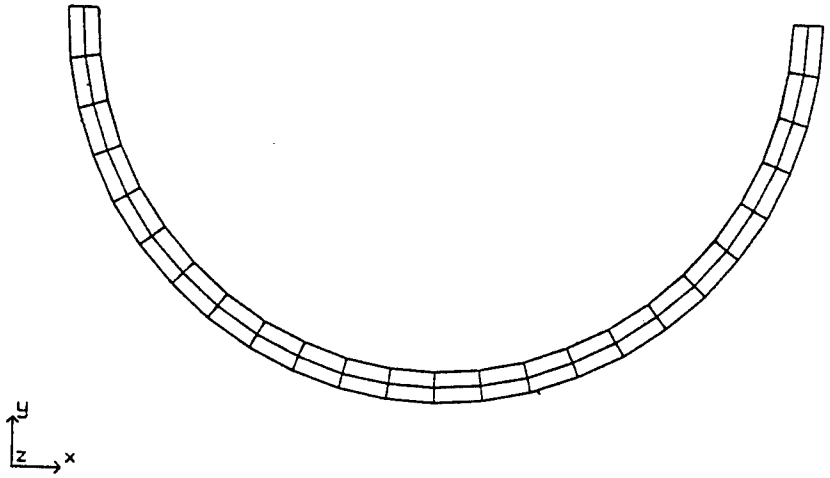

Figure 2b. Finite element model of infinite cylinder

IV. ANALYSIS OF ONE-DIMENSIONAL MODEL

A. FREE END BOUNDED BY AIR

1. Wave Propagation Through Elastic Material

Kolsky [Ref. 11] asserts that stress wave propagation can be defined with the equations of motion expressed in terms of particle displacement. The three-dimensional displacement components, u, v, and w in the x, y, and z directions, respectively, satisfy the following equations:

$$\rho \frac{\partial^2 u}{\partial t^2} = (\lambda+\mu) \frac{\partial \Delta}{\partial x} + \mu \nabla^2 u \tag{5}$$

$$\rho \frac{\partial^2 v}{\partial t^2} = (\lambda+\mu) \frac{\partial \Delta}{\partial y} + \mu \nabla^2 v \tag{6}$$

$$\rho \frac{\partial^2 w}{\partial t^2} = (\lambda+\mu) \frac{\partial \Delta}{\partial z} + \mu \nabla^2 w \tag{7}$$

where: ρ = density of the solid containing the stress wave

Δ = dilatation, given by the following expression:

$$\Delta = \frac{\partial u}{\partial x} + \frac{\partial v}{\partial y} + \frac{\partial w}{\partial z} \tag{8}$$

λ = Lamé's constant, which is equal to

$$\lambda = k + \frac{2\mu}{3} \tag{9}$$

k = bulk modulus of the structure

μ = material shear modulus

∇^2 = Laplace operator

Considering only one-dimensional displacement in the x-direction, the rest of this discussion will pertain to equation (5) only. The solution to this equation for an extended medium corresponds to both dilatational and distortional waves. Dilatational wave propagation is parallel to stress wave motion while distortional waves are

perpendicular to this motion. Due to the one-dimensional restriction placed upon the model elements, only longitudinal vibrations will be retained. Therefore, displacement will take the form of alternating element contraction and extension with no lateral displacement along the main axis of the model.

2. Homogeneous Elastic System

First consider a point just on the structure side of the interface of a model with the coating and structure of the same material. The common material is aluminum, a metal with good elastic behavior. In other words, the entire system is a homogeneous material. The ratio of the coating stiffness, E_c, to the structure stiffness, E_s, is unity. The term system will be used to describe the coating and structure as one integral unit. The free end of the system exposed to the air medium is subjected to an unit step pressure wave. The incident pressure wave will travel the length of the system without dispersion at rate c_o, the velocity of stress wave propagation. The compression wave will propagate through the uniform material directly to the fixed end of the structure (Figure 3a). There is no reflected wave at the interface between the coating and the structure because the characteristic impedance, ρc_o, between the coating and structure is identical.

The pressure wave will produce varying degrees of displacement as it is transmitted through the system. The nodal displacement will be the largest at the free end and will decrease towards the fixed boundary. If the displacement created by the incident wave is expressed as:

$$u_1 = F(c_o t - x) \qquad (10)$$

and the displacement created by a reflected wave is given by:

$$u_2 = f(c_o t + x) \qquad (11)$$

then from these above equations, the total displacement is:

$$u_1+u_2 = F(c_o t-x)+f(c_o t+x) \qquad (12)$$

When the pressure wave is reflected from a fixed surface, the boundary condition is one of zero-displacement. Due to this boundary condition, the above equations can be simplified to:

$$f(c_o t+x_o) = -F(c_o t-x_o) \qquad (13)$$

where x_o is the coordinate value at the fixed boundary. Thus the particle displacement behind the reflected wave, u_2, is equal and opposite to the particle displacement behind the incident wave. The pressure wave is completely reflected at a perfectly rigid or fixed boundary only both the direction of displacement and propagation are reversed. In other words, the stresses produced by the step wave are additive at the fixed end and the resultant stress is double the value of stress created by the incident wave.

The reflected pressure wave travels along the length of the system to the free end, the point of origin (Figure 3b). When the wave reaches the free end, it will be again reflected. However, the boundary condition here is one of no stress normal to the end face of the system. The characteristic impedance of the air is negligible in comparison to the coating. The stress produced by the two waves in the direction of propagation is given as follows:

$$E\frac{\partial u_1}{\partial x} \quad together\ with \quad E\frac{\partial u_2}{\partial x} \qquad (14)$$

The cumulative stress at the free end is given by the following equation:

$$E\left(\frac{\partial u_1}{\partial x}+\frac{\partial u_2}{\partial x}\right) = E[-F'(c_o t-x)+f'(c_o t+x)] \qquad (15)$$

If the free end is stress-free, then the above equation is simplified to:

$$-F'(c_o t-x)+f'(c_o t+x) = 0 \qquad (16)$$

and the compressive wave is reflected as a like tensile wave.

The tensile wave relieves the additional stress caused by the propagation of the reflected compressive wave (Figure 3c). It undoes some of the stress caused by the passage of two compressive waves across the system. When this tensile wave reaches the fixed boundary, it is reflected as a tensile wave of equal magnitude (Figure 3d). The tensile wave undoes the remaining compressive stress giving the structure a zero-stress state. This cycle is identically repeated throughout the duration of the pressure wave. Figure 4 summarizes the events described above at a point on the structure.

3. Elastic Coating Less Stiff Than Structure

The previous discussion dealt with a homogeneous coating-structure system. In reality, there will be a difference in the characteristic impedance between the coating and the underlying structure due to the use of dissimilar materials. Consider the case where the coating maintains the same material properties of aluminum, but the stiffness is reduced by a factor of 10 (i.e., $E_c/E_s = 0.1$). This rather fictitious material is used to understand the wave phenomenon for a system having two different characteristic impedances. When the system is impacted by an external pressure wave at the free surface, the resulting compressive stress wave now will interact at the interface between the coating and structure.

The wave strikes the interface and produces two waves: reflected and transmitted waves. To maintain stress equilibrium at the interface, a transmitted compressive wave (C) of equal to the incident (c) plus the reflected wave (c^*) propagates through the structure (Figure 5a). This transmitted wave, which is of greater magnitude than the initial wave, will travel at a speed about three times faster than the reflected wave, which is of smaller magnitude than the initial

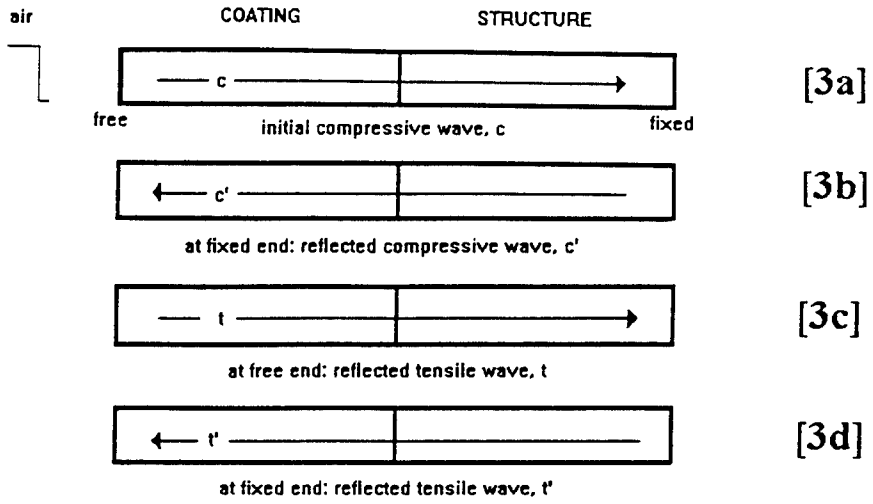

Figure 3. Homogeneous aluminum system (E_c/E_s = 1) subjected to unit step pressure wave

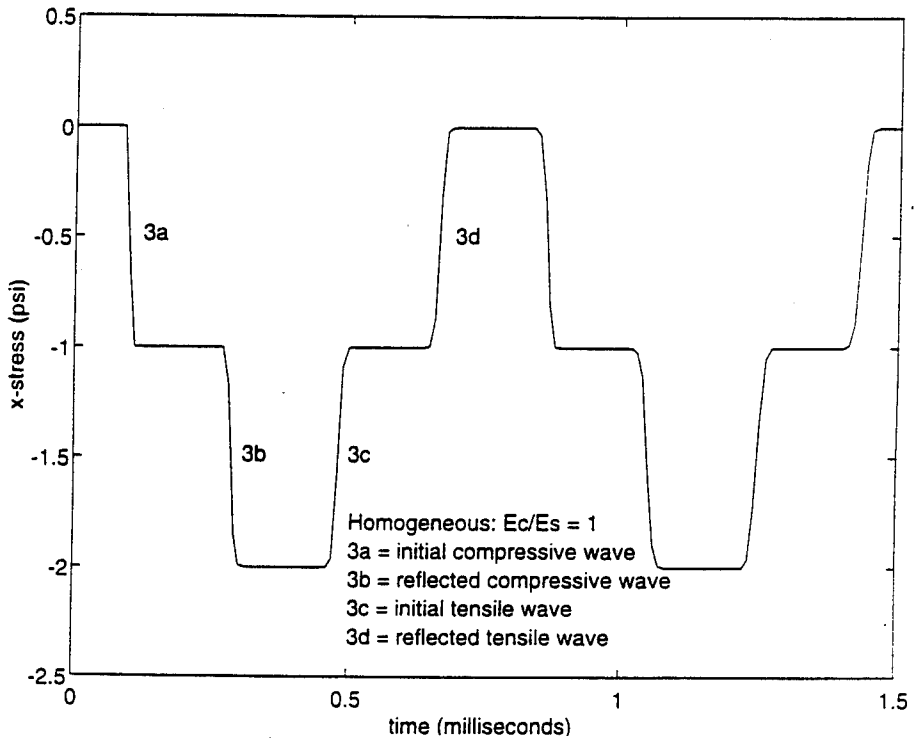

Figure 4. Stress history for homogeneous system at a point near the interface on the structure

wave, due to the larger elastic modulus of the structure with the same density. The transmitted wave is reflected back into the structure at the fixed end as a compressive wave (C') of equal magnitude (Figure 5b). The reflected wave propagating back towards the coating strikes the interface. Since it encounters a less stiff material, the stress wave is reflected back into the structure as a tensile wave (T), which relieves some of the net compressive stress in the structure (Figure 5c). At the same time a compressive stress wave (c') of very small magnitude is transmitted into the coating. The tensile wave in the structure is reflected at the fixed boundary as a returning tensile wave (T') of equal magnitude (Figure 5d). This returning wave strikes the interface producing a reflected compressive wave (C'') into the structure and a transmitted tensile wave (t') into the coating (Figure 5e). The compressive wave is reflected as an identical compressive wave (C''') at the fixed end (Figure 5f). This compressive wave strikes the interface producing transmitted compressive (c''') and reflected tensile (T'') waves. The reflected tensile wave is combined with another tensile wave transmitted from the coating. The latter wave (t^*) is the initial compressive wave (c^*), which was reflected at the free end (Figure 5g). The resultant tensile wave is reflected as a tensile wave (T''') at the fixed end. These waves relieve the stress to nearly zero (Figure 5h). Figure 6 summarizes the above events at a point on the structure.

The same behavior is seen in systems with coatings 100 and 1000 times less stiff. The time of a complete cycle from compression to release increases with decreasing coating stiffness since the less stiff coating has a smaller acoustic velocity. The number of small magnitude compression and tension cycles in the structure also increases. The net stress values remain constant, but the magnitude of the transient spikes increases with decreasing coating stiffness (Figure 7).

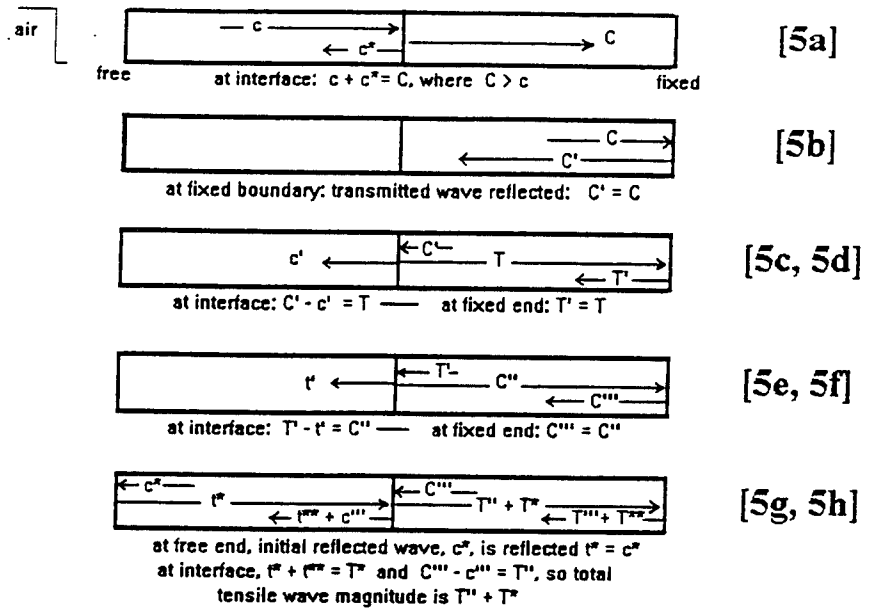

Figure 5. System with aluminum coating 10 times less stiff (E_c/E_s = 0.1) subjected to unit step pressure wave

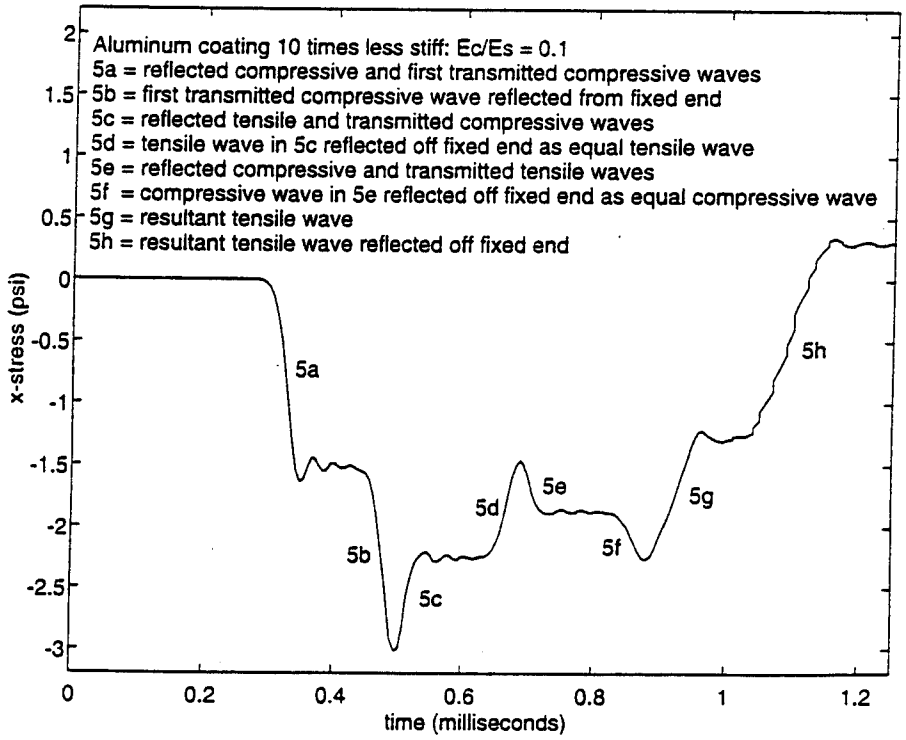

Figure 6. Stress history at a point near interface on the structure with coating 10 times less stiff (E_c/E_s = 0.1)

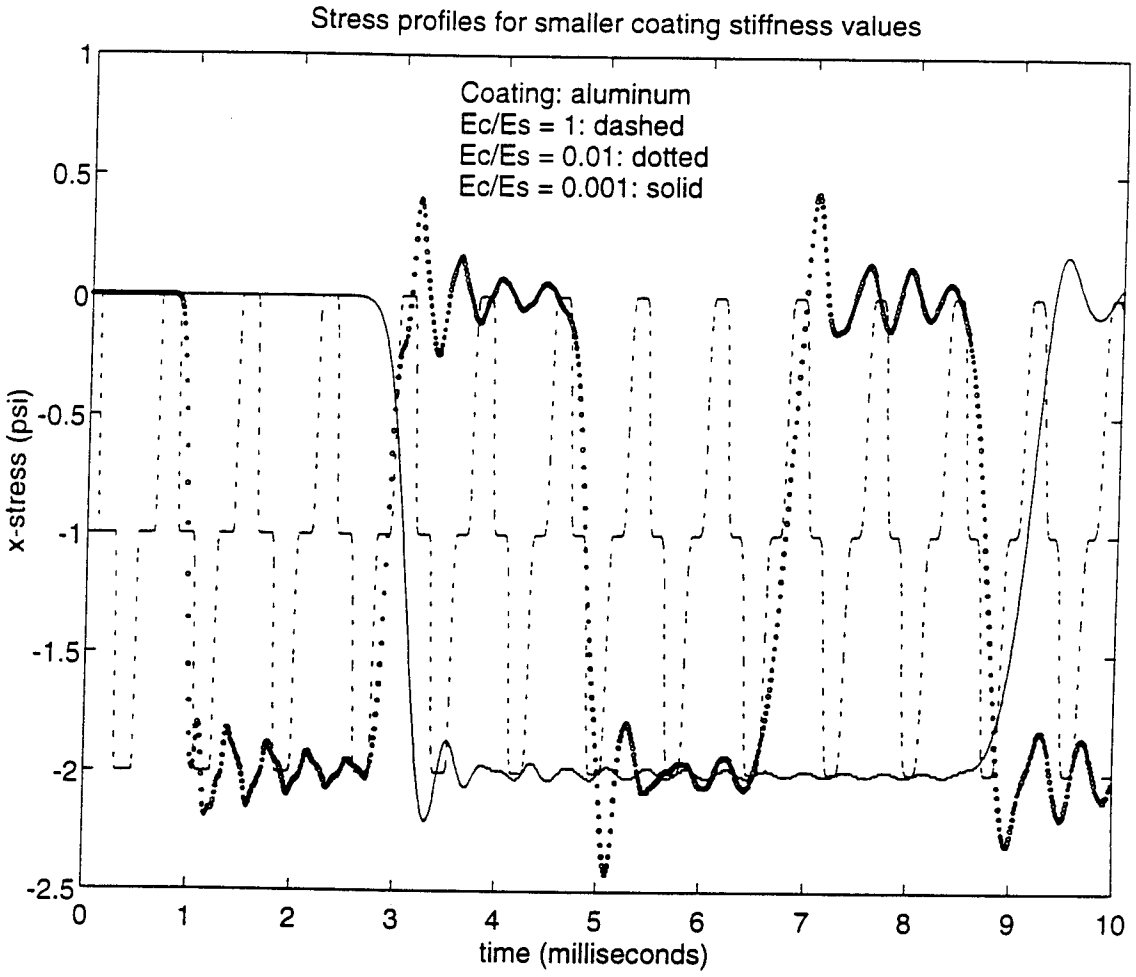

Figure 7. Stress profiles at a point near the interface on the structure for aluminum coated structures: homogeneous, $E_c/E_s = 0.01$, $E_c/E_s = 0.001$

4. Elastic Coating Stiffer Than Structure

If the stiffness of the coating is increased by factor of 10 (i.e., $E_c/E_s = 10$), the pressure wave from the air propagating through the system has a different dynamic response. Since the structure is less stiff than the coating, the reflected wave (t) at the interface is tensile while the transmitted wave (C) is compressive (Figure 8a). The reflected tensile wave travels approximately three times faster in the coating due to a larger elastic modulus in the coating with the same density. This wave is reflected at the free end as a compressive wave (c') of equal magnitude. This reflected wave interacts at the interface producing a weaker reflected tensile wave (t') into the coating and a weaker second compressive wave (C') into the structure (Figure 8b). The process repeats itself with an even weaker third compressive wave (C'') into the structure (Figure 8c). In the interim, the first compressive wave transmitted into the structure (C) is reflected at the fixed boundary as a compressive wave thereby increasing the net compressive stress of the structure (Figure 8d). The second and third transmitted waves follow in succession and contribute to the net compressive stress in the structure.

The competing effects of alternating compression and tension are observed until the final in a series of tensile waves (T^*) is transmitted to the structure, which relieves the compressive stress completely. Figure 9 depicts the stress history of the system with an aluminum coating 10 times stiffer than the structure.

There is little difference in the stress resulting from the coating stiffness increased by a factor of 100 or even 1000 (Figure 10). The stiffer coating example is used as a means of understanding the mechanics of stress wave behavior in a solid. In general, the coating will be less stiff than the structure it is designed to protect.

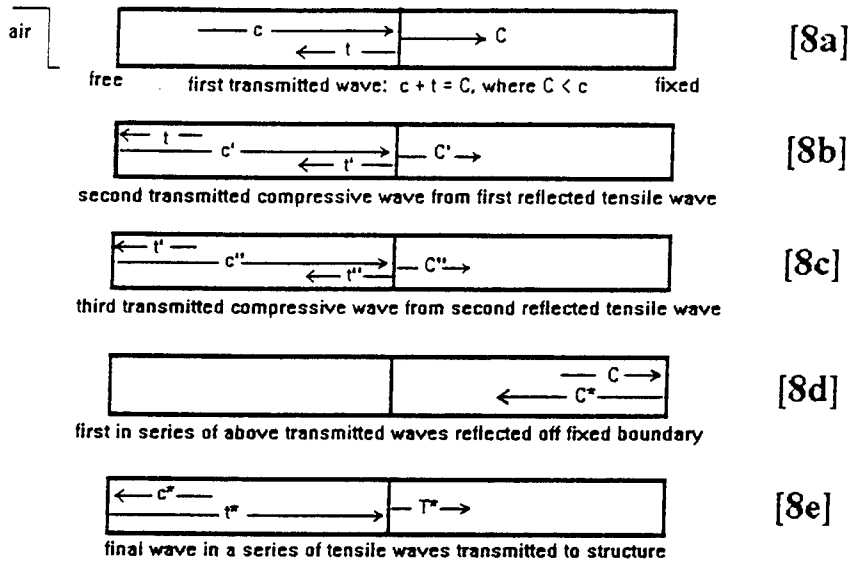

Figure 8. System with aluminum coating 10 times stiffer (E_c/E_s = 10) subjected to unit step pressure wave

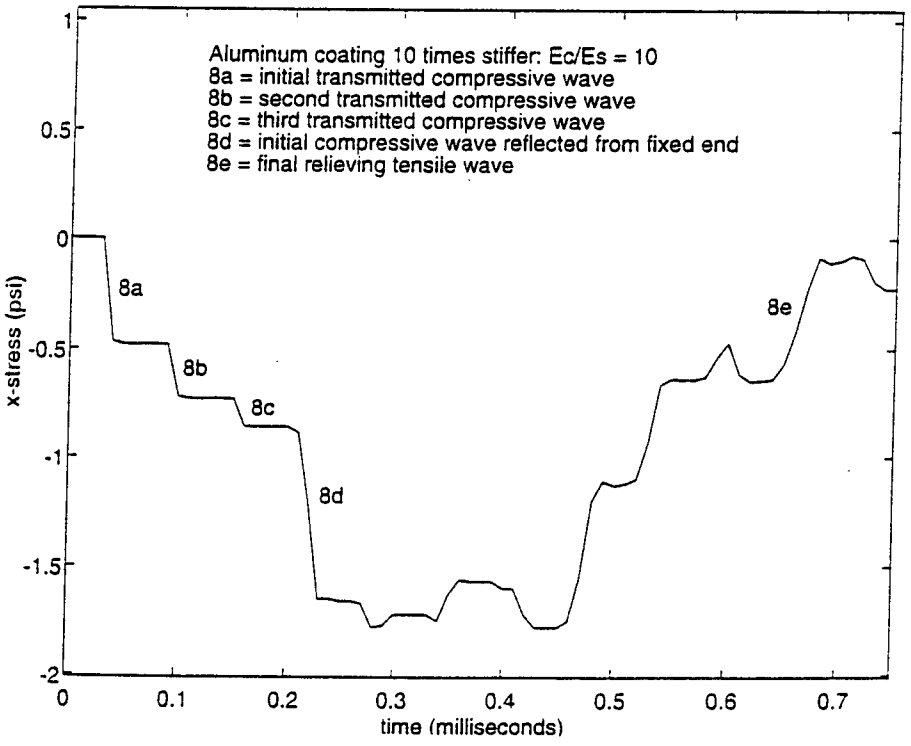

Figure 9. Stress history at a point near the interface on structure with coating 10 times stiffer (E_c/E_s = 10)

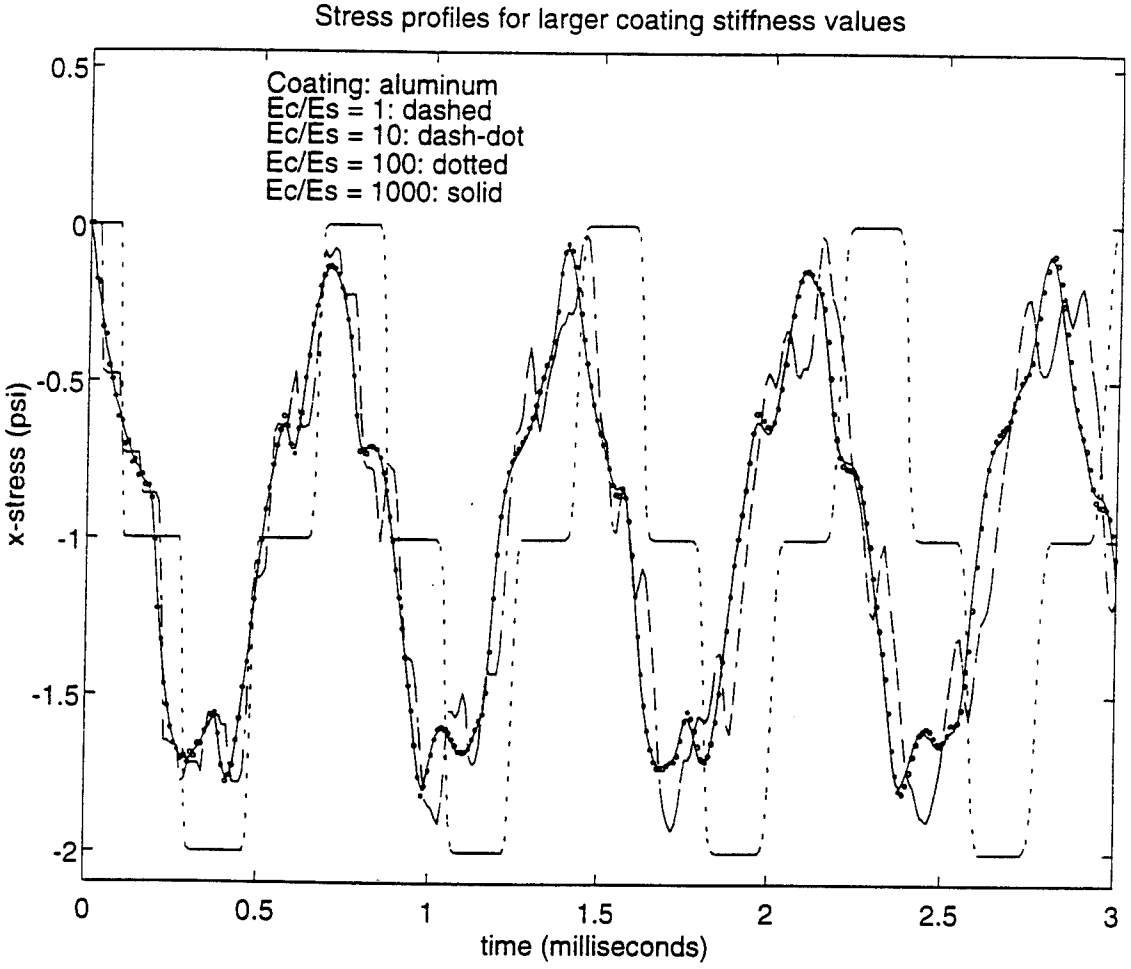

Figure 10. Stress profile at a point near the interface on the structure for aluminum coated structures: homogeneous, $E_c/E_s = 10$, $E_c/E_s = 100$, $E_c/E_s = 1000$

5. Effect of Elastic Coating Characteristic Impedance

The previous sections examined the dynamic response of the coated structure by altering only the stiffness of the coating. However, in doing so, only one variable (c_o) of the coating's characteristic impedance, ρc_o, was changed while the other variable (ρ) remained constant. The degree of wave propagation between the coating and structure depends upon the relative values of their characteristic impedances.

The speed of sound, c_o, in an elastic material is a function the stiffness, E, and the density, ρ, of the material as given in the following equation:

$$c_o = \sqrt{\frac{E}{\rho}} \tag{17}$$

Therefore, the characteristic impedance relates the material stiffness and density as follows:

$$\rho c_o = \rho\sqrt{\frac{E}{\rho}} = \sqrt{\rho E} \tag{18}$$

Thus the characteristic impedance of a homogeneous system equates the coating impedance to the structure impedance as:

$$\rho_C E_C = \rho_S E_S \tag{19}$$

The mismatch of impedances between the coating and structure influences the response of the stress wave at the coating-structure interface. For example, consider the following three cases using the same fixed-free one-dimensional system impacted by a unit step pressure wave: The first case examines the stress induced in a structure coated with an elastic material having an identical impedance. The second case studies the response of a system where the coating impedance is half the structure impedance. The coating impedance is double the structure impedance in the third case.

In the first case, the stiffness of the coating is increased by a factor of two while the density is reduced by a factor of two. The coating impedance, therefore, remains the same as the structure impedance. The magnitude of stress induced in the structure is identical to the resultant stress in the homogeneous system observed previously. There is no stress wave interaction at the interface; so the wave traverses the entire system without dispersion until it is reflected at the fixed boundary.

In the second case, the stiffness of the coating is increased by a factor of two while the density is decreased by a factor of four. Thus the impedance of the coating is reduced by a factor of two. The initial compressive wave strikes the interface causing a compressive wave to be reflected back into the coating. A compressive wave equal in magnitude to the sum of the initial and reflected compressive waves is transmitted into the structure. The transmitted compressive wave is of greater magnitude than the initial compressive wave. It raises the stress of the underlying structure as was observed when the coating stiffness was reduced by a factor of 10.

The stiffness of the coating is reduced by a factor of two while the density is increased by a factor of four in the final case. The coating impedance is increased by a factor of two over the structure impedance. The initial compressive wave strikes the interface causing a tensile wave to be reflected back into the coating. A net compressive wave equal to the sum of the initial compressive and the reflected tensile waves is transmitted into the structure. The weaker transmitted wave will result in a smaller stress state of the structure. This phenomenon was observed when the stiffness of the coating was increased by a factor of 10.

Thus the observation of wave propagation at the coating-structure interface is a practical method of determining the overall stress level in the structure for a coating with a

given impedance. A coating with a characteristic impedance less than that of the structure will induce a higher magnitude of stress in the structure; conversely, a coating of larger impedance will induce a smaller stress magnitude in the structure. Figure 11 summarizes the response of the three cases studied above.

The internal energy of the structures for each of the three cases is given in Figure 12. A smaller value of internal energy present in the structure accompanies the system with a higher coating impedance or stiffer coating with the same density.

6. Nearly Incompressible Rubber Coating

Up to this point, the coating and structure have had similar characteristics; only the impedance of the coating had been varied. A greater degree of complexity is added when the coating material type is changed altogether.

A more realistic structural coating entails substituting the elastic coating with a nearly incompressible tread stock rubber coating. The unit step pressure wave transmitted to the system will now first transit the rubber coating, which will have a significant impact on the wave characteristics when it reaches the structure. The response may not be as predictable.

In the parametric study, an observation of the stress response shows that the tread stock rubber coating produces larger magnitudes of stress in the aluminum structure when compared to that in the homogeneous structure (Figure 13). The initial compressive wave is alternately reflected at the fixed end and re-reflected at the interface in a series of compressive and tensile waves. The stress wave alternates compressive and zero-stress states much slower than the aluminum coated models causing the structure to remain in a compressive stress state for a longer period of time. The rubber raises the internal energy of the structure to a level much higher than compared to the elastic coating (Figure 14).

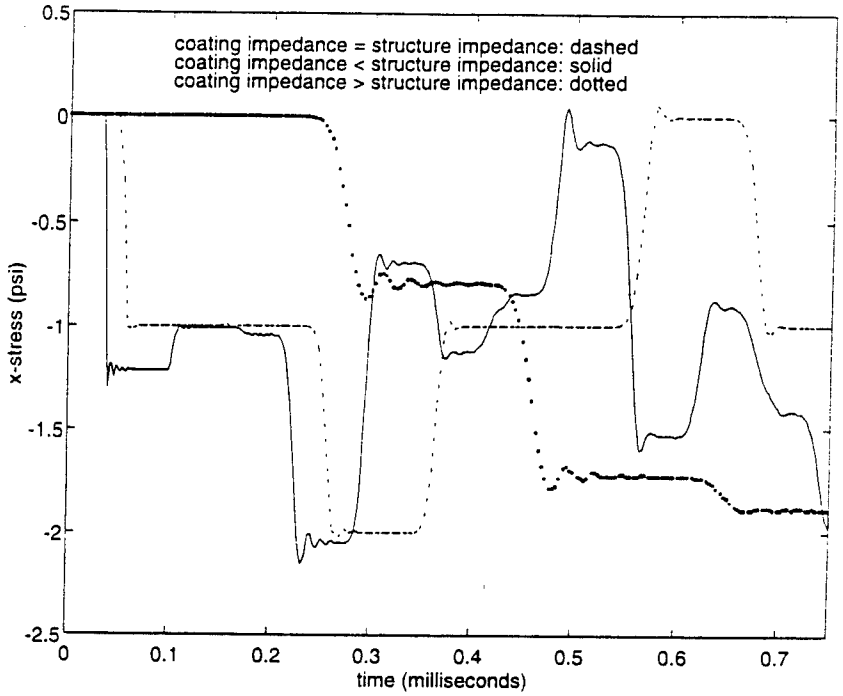

Figure 11. Stress history at a point near the interface on the structure with identical and unequal coating and structure impedances

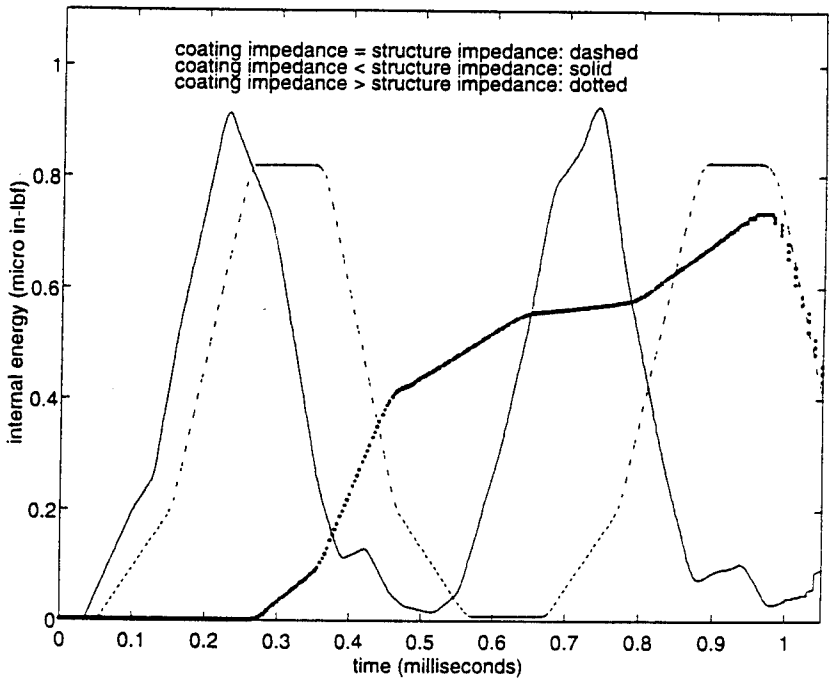

Figure 12. Internal energy of structure for systems with identical and unequal coating and structure impedances

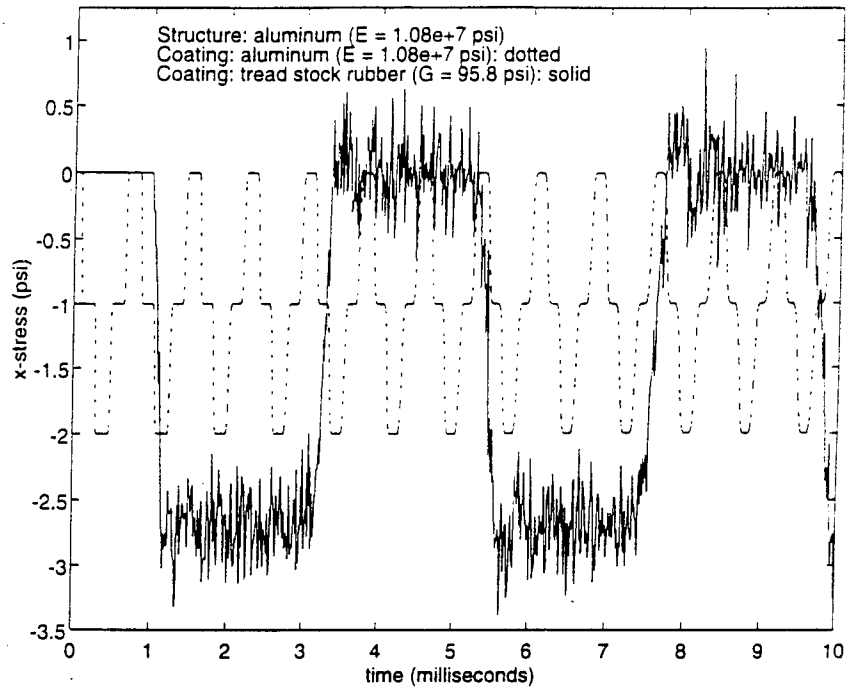

Figure 13. Stress profiles at a point near the interface on the structure comparing aluminum (E = 1.08e+7 psi) and tread stock rubber (G = 95.8 psi) coated systems

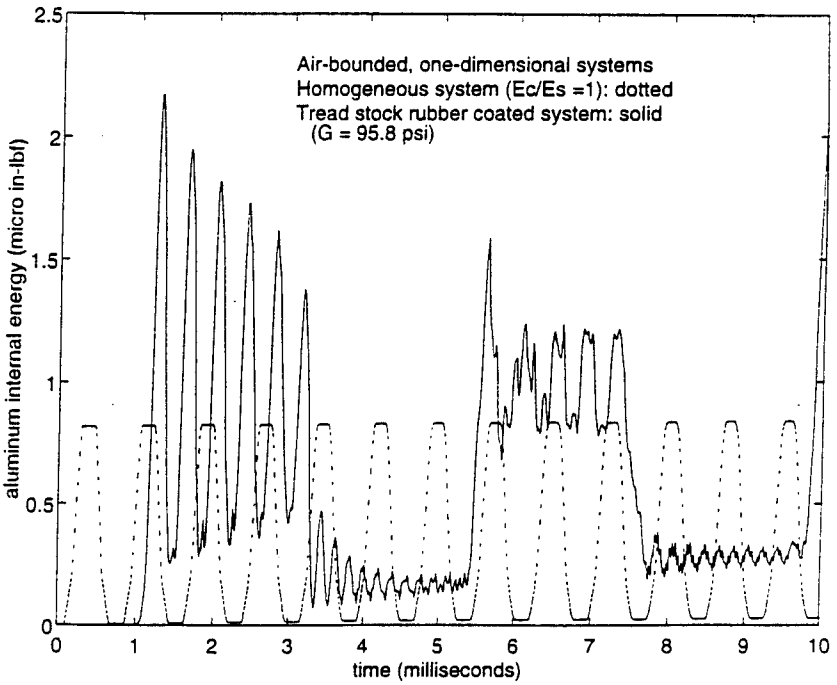

Figure 14. Comparing internal energy of aluminum structure using elastic and rubber coatings

Suppose the properties of tread stock rubber remain constant only the coating shear modulus is increased by a factor of 10. Both the average stress wave magnitude and periodicity decrease, but the stress at a point in the rubber coated structure exceeds the stress in the homogeneous aluminum structure (Figure 15). In other words, the dynamic response is adverse. If the rubber shear modulus is increased by a factor of 100, the dynamic response of the rubber coated structure is favorable when compared to the homogeneous aluminum response (Figure 16); the stress state is smaller.

A "threshold value" for a shear modulus of the rubber coating is apparent between 958 psi and 9580 psi. The threshold value is defined as the particular rubber coating shear modulus value for the system which possesses equivalent magnitudes of stress in the underlying structure as the homogeneous or uncoated structure subjected to the same shock conditions. Further investigation reveals that a rubber shear modulus of 6000 psi and greater will render a favorable dynamic response for the rubber coated, one-dimensional, air-bounded model (Figure 17). The threshold value, however, is only applicable for a certain geometry of the structure and the coating; its magnitude is case-dependent.

The elastic-coated model demonstrated a relationship between the coating impedance and the degree of wave propagation (or energy exchange) at the interface. This concept can be extended to the rubber-coated model. However, the stress wave interaction with the rubber as it traverses the system and response of the wave at an interface of two dissimilar materials are not as clearly defined.

The rubber threshold value of shear modulus was determined to be greater than 6000 psi for the above model. There will be a coating impedance, ρc_o, associated with the threshold value as well. Thus there is a "critical difference" in the impedance values between the rubber coating and elastic

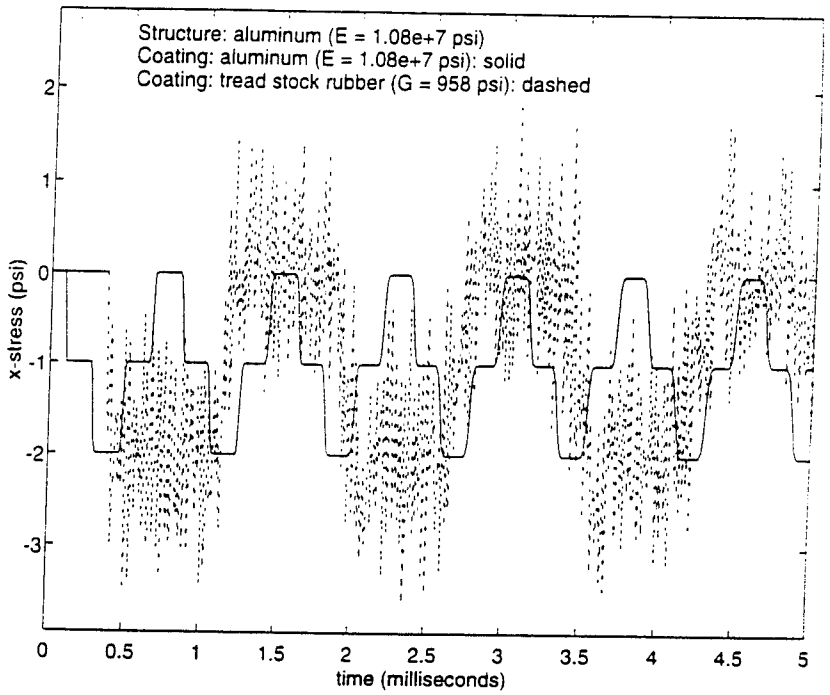

Figure 15. Comparing stress profiles at point near interface on structure for aluminum versus tread stock rubber coating (G = 958 psi)

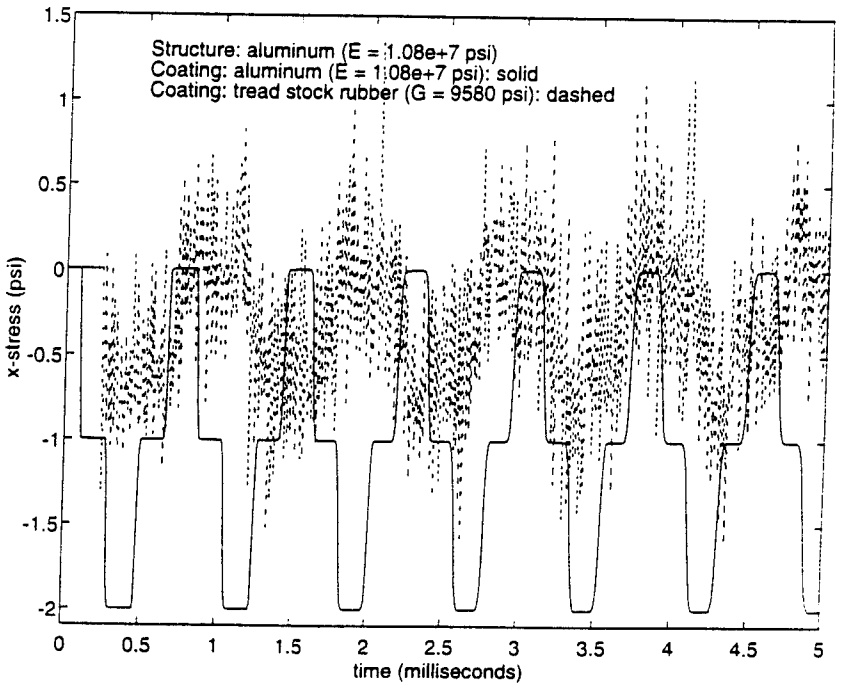

Figure 16. Comparing stress profiles at point near interface on structure for aluminum versus tread stock rubber coating (G = 9580 psi)

structure. In other words, the threshold value can be defined in terms of a critical difference between the coating and structure impedances.

If the impedance difference exceeds the critical difference, the dynamic response of the system will be more adverse as compared to the homogeneous or uncoated system. For example, when the rubber shear modulus was either 95.8 psi or 958 psi, a higher stress level was induced in the underlying structure. But a rubber coating with a shear modulus of 9580 psi resulted in a favorable response. The impedance difference in the latter case is less than the critical difference.

Suppose the coating impedance is set equal to the coating impedance when the shear modulus is 6000 psi. However, in this case, both the density and shear modulus are changed. Unlike for the elastic coating, the equivalent impedance must be found by trial and error. The speed of wave propagation is different, but the stress magnitude remains unchanged (Figure 18). Consider the case where the coating maintains G = 6000 psi only the rubber density is first increased then decreased by a factor of two rendering a smaller and larger impedance, respectively. The stress increases with a decrease in the impedance creating a difference which exceeds the critical difference. The results are given in Figure 19 and Figure 20.

In general, the stress induced in the structure increases with rubber coatings of smaller characteristic impedances. The smaller impedance is indicative of a less stiff or softer coating. The softer rubber appears to concentrate stress wave energy within the structure. For example, an increase in the internal energy accompanies a decrease in the rubber shear modulus (Figure 21). This excess energy remains trapped within the structure. The result is a higher stress state, which elevates the structural material closer to yield stress limits. In more extreme instances, plastic deformation and failure of the structure ensues.

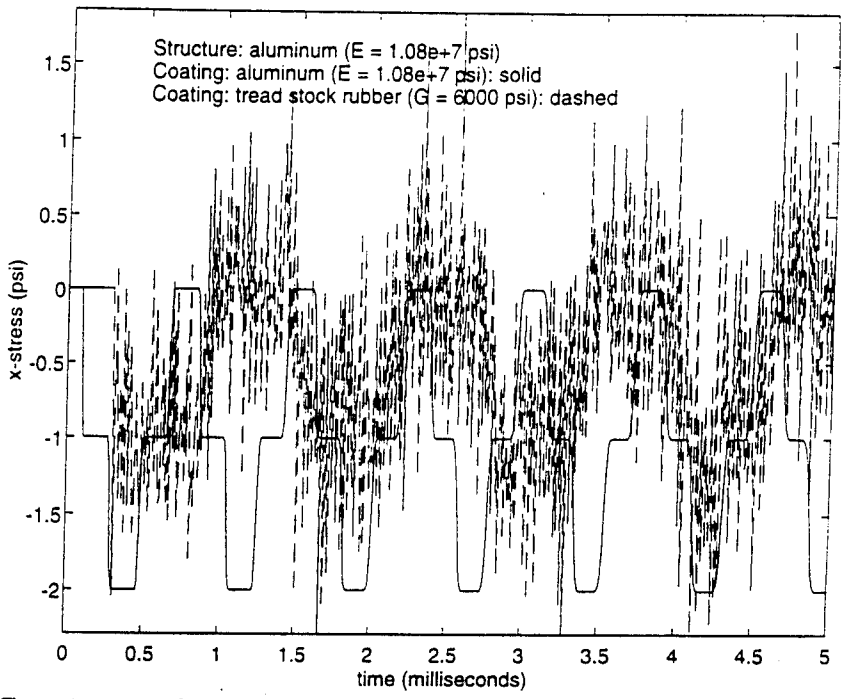

Figure 17. Comparing stress profiles at point near interface on structure for aluminum versus tread stock rubber coating (G = 6000 psi)

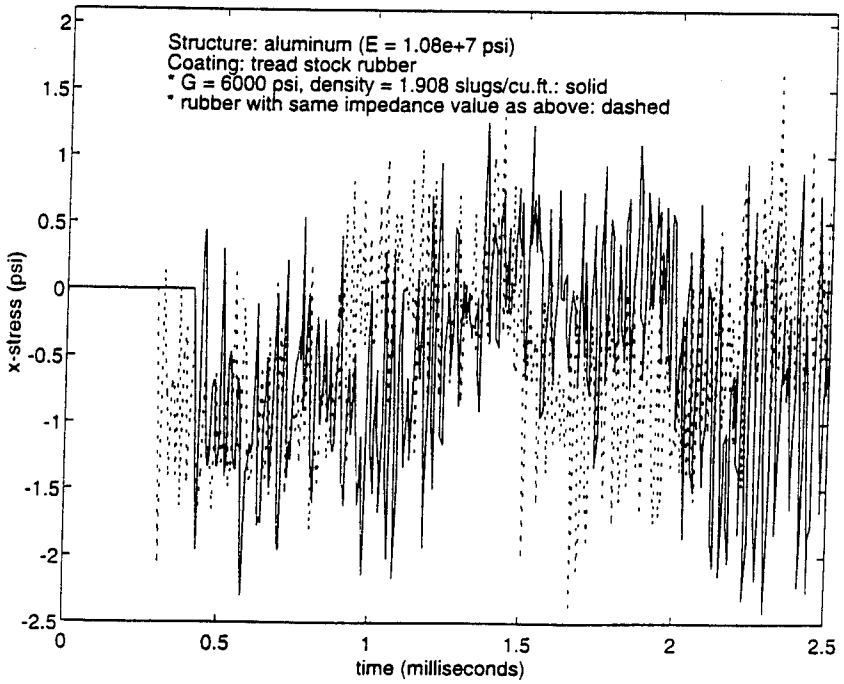

Figure 18. Comparing stresses at point on structure for rubber-coated systems with identical impedances

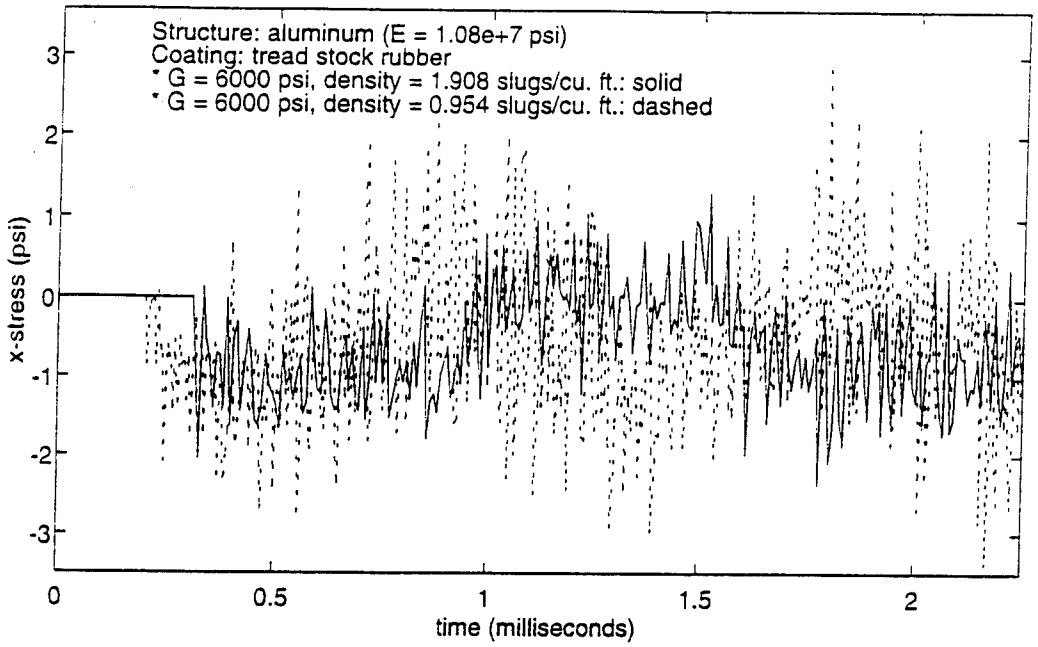

Figure 19. Comparing stresses at point on rubber-coated structures each of different densities

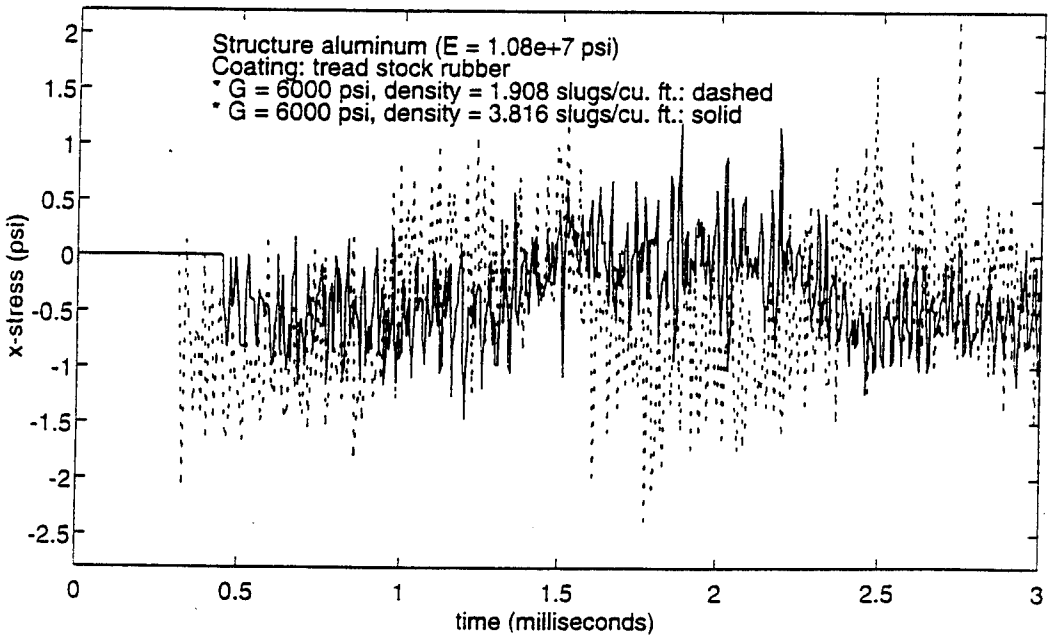

Figure 20. Comparing stresses at point on rubber-coated structures each of different densities

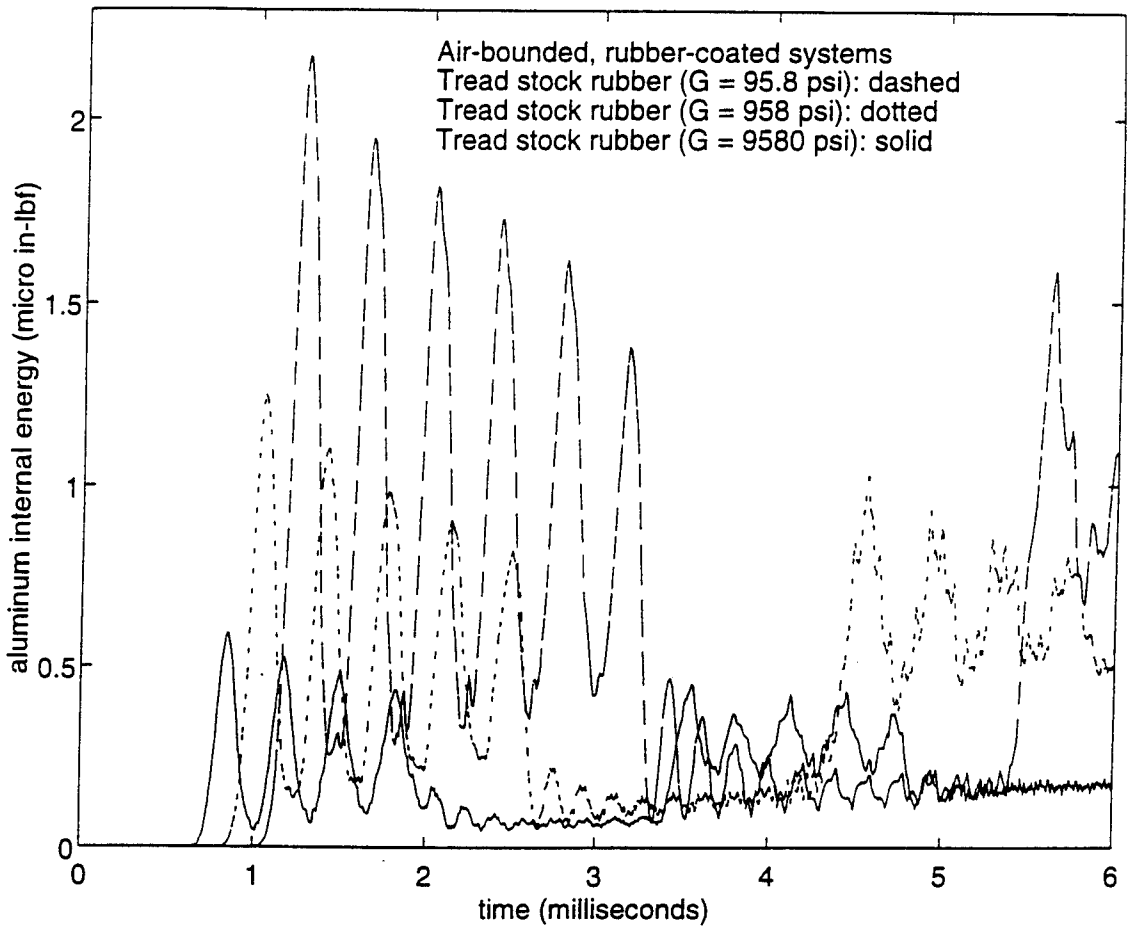

Figure 21. Comparing internal energy of structure with tread stock rubber coating of varying shear moduli: G = 95.8 psi, G = 958 psi, and G = 9580 psi

B. FREE END BOUNDED BY WATER

Previously, all the systems studied have had the free end of the system bounded by an air medium. The scope of the analysis now shifts to a more realistic application by observing a water-bounded system subjected to the same conditions previously prescribed. The dynamic response will be altered at the subsequent times after impact.

The characteristic impedance of air is essentially negligible. Thus there is little wave energy transmission to the air from the system. A compressive wave interacting with the free end will be reflected as a tensile wave of nearly the same magnitude and vice-versa. The introduction of a water medium at the free end alters the dynamic response of the system.

The water is a material with a characteristic impedance approximately 3600 times that of air. Stress wave energy will be more readily transmitted from both the structure and the coating to the water medium. Therefore, waves reflected at the free end will now be smaller in magnitude.

As shown in the following derivation, the velocity at any point on the structure is proportional to the stress. As a result, the nodal velocity at a point on the structure is used to compare the dynamic response of the system bounded by water for various coatings.

For a one-dimensional element on the structure, recall from (12) that the total displacement of the element due to the pressure wave is expressed as:

$$u = F(c_o t - x) + f(c_o t + x)$$

If the wave is travelling in the direction of increasing x ,

$$u = F(c_o t - x) \qquad (20)$$

then differentiate both sides with respect to displacement, x, to get the following:

$$\frac{\partial u}{\partial x} = -F'(c_o t - x) \tag{21}$$

If (20) is differentiated with respect to time, t, then:

$$\frac{\partial u}{\partial t} = c_o F'(c_o t - x) \tag{22}$$

From (21) and (22) above, the following expression is derived:

$$\frac{\partial u}{\partial t} = -c_o \frac{\partial u}{\partial x} \tag{23}$$

and, finally, from equation of equilibrium, the result is expressed as:

$$\sigma_{xx} = -\left(\frac{E}{c_o}\right) \frac{\partial u}{\partial t} = -\rho c_o \frac{\partial u}{\partial t} \tag{24}$$

This equation gives the relationship between the stress at any point on the structure and the particle velocity with the characteristic impedance as the proportionality constant. Henceforth, the dynamic response of the one-dimensional, water-bounded systems will be given in terms of the nodal velocity of a point on the structure.

1. Elastic Coating

Consider the homogeneous system, that is one using identical material for the coating and structure, subjected to a unit step pressure wave at the free end. The velocity response of a node on the structure side of the interface resembles that of the homogeneous system exposed to air. However, even though the two velocity profiles have identical time periods, the velocity of the water-bounded system decays to zero as time elapses (Figure 22). A similar response results regardless of the coating stiffness (Figures 23, 24, 25, 26). The air-bounded system cycles at the same amplitude throughout the duration of the pressure pulse. The water

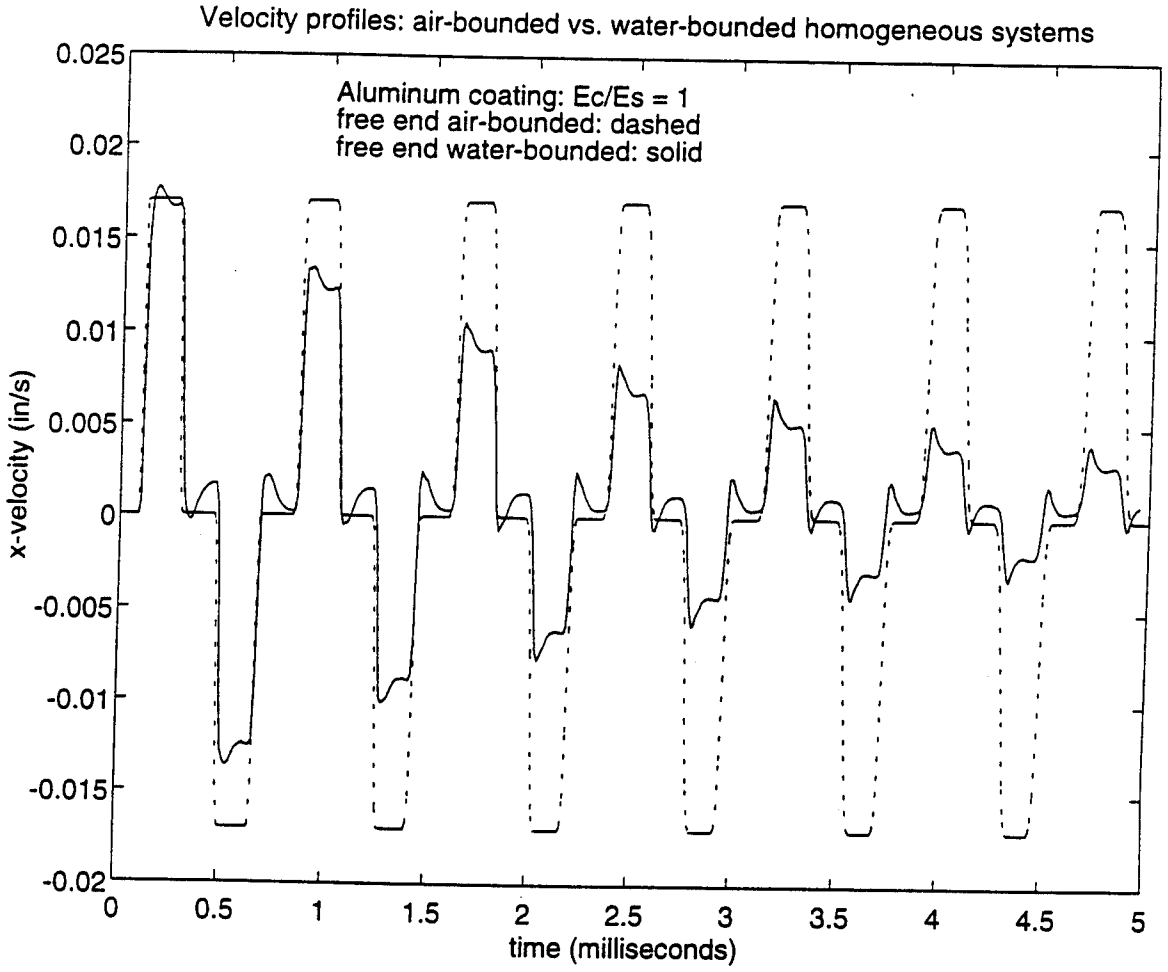

Figure 22. Comparing velocity profiles at a point near the interface on structure for air-bounded versus water-bounded homogeneous systems

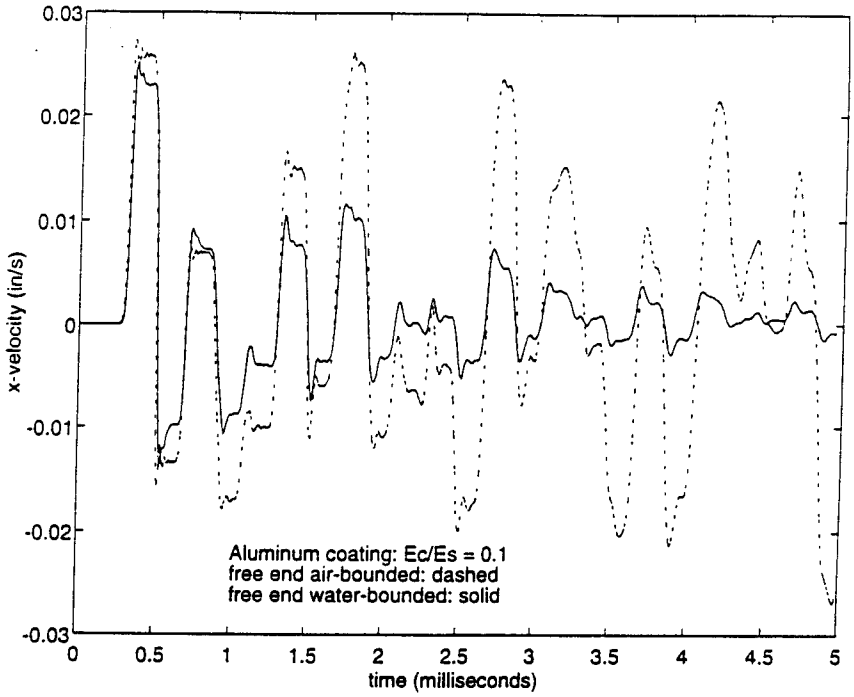

Figure 23. Comparing velocity profiles at a point near interface on structure for air-bounded vs. water-bounded coatings (E_c/E_s = 0.1)

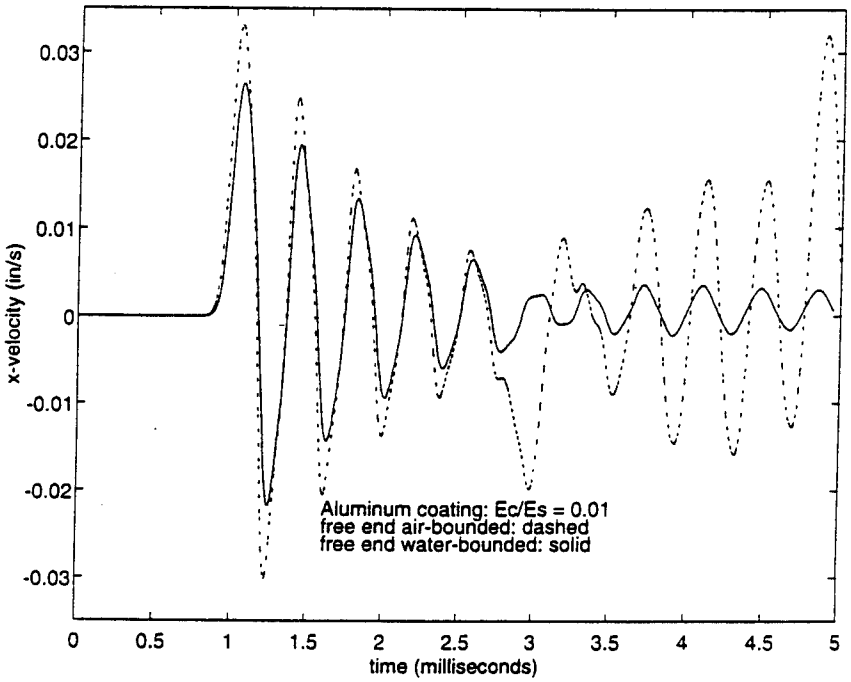

Figure 24. Comparing velocity profiles at a point near interface on structure for air-bounded vs. water-bounded coatings (E_c/E_s = 0.01)

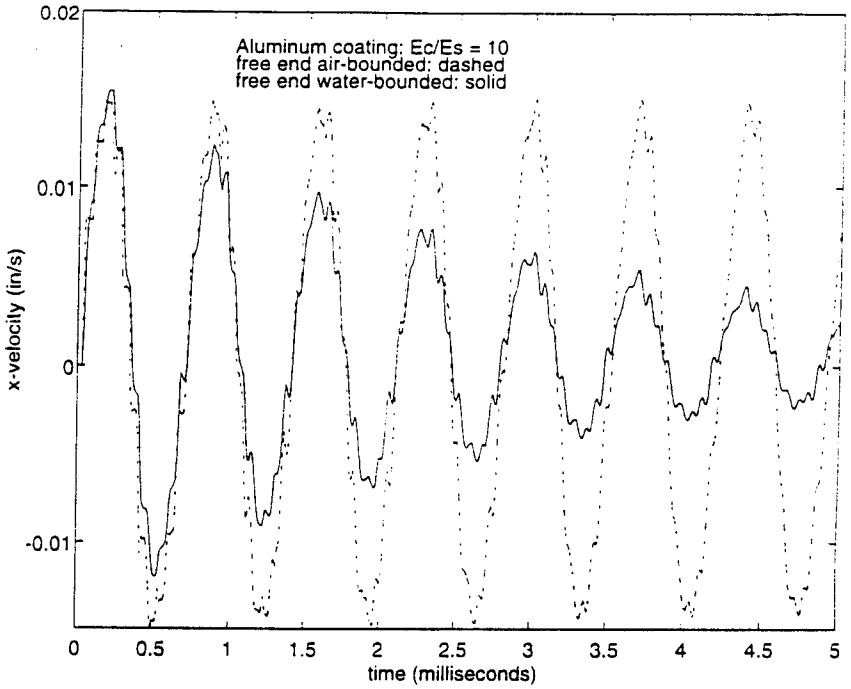

Figure 25. Comparing velocity profiles at a point near interface on structure for air-bounded vs. water-bounded coatings (E_c/E_s = 10)

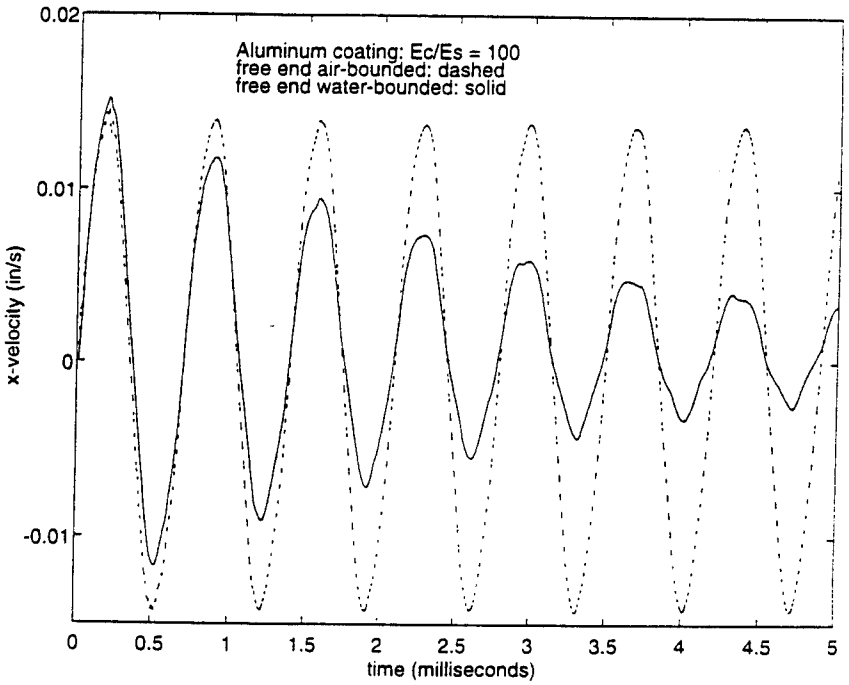

Figure 26. Comparing velocity profiles at a point near interface on structure for air-bounded versus water-bounded coatings (E_c/E_s = 100)

dampens out a portion of the stress wave energy; this allows the system to return to a lower energy state as time goes on.

The impedance of the coating influences the nodal velocity of the structure. This velocity is indicative of the stress state in the structure; a higher stress state is characterized by a higher velocity. The peak nodal velocity increases while the period between successive peaks decreases with decreasing elastic coating impedance (Figures 27, 28). The softer elastic coating inhibits release of stress wave energy from the structure to the surrounding water medium. The excess energy is manifested in the form of higher nodal velocities and stresses in the underlying structure. Therefore, a higher stress state accompanies an elastic coating with a smaller characteristic impedance.

2. Nearly Incompressible Rubber Coating

Comparing the velocity profile of the air-bounded to the water-bounded tread stock rubber coated system, there is a distinct difference in the velocity of a structural node just inside the coating-structure interface. The nodal velocity of the air-bounded system is greater. Thus the air-bounded system has a higher stress magnitude regardless of the rubber shear modulus (Figure 29). This higher stress state is indicative of less stress wave energy being released to the air when compared to the energy dissipation to the water.

As previously discussed, a point on the structure with an elastic coating has a velocity profile decreasing with time. On the other hand, the response of the rubber coated system is not as smooth or predictable. The compressible rubber coating yields an erratic nodal velocity characterized by alternating peaks and nadirs of unequal magnitude (Figure 30).

Increasing the shear modulus of the tread stock rubber by a factor of 10 results in a smaller, more refined velocity profile. However, a higher nodal velocity in the structure indicates that this dynamic response is worse than the

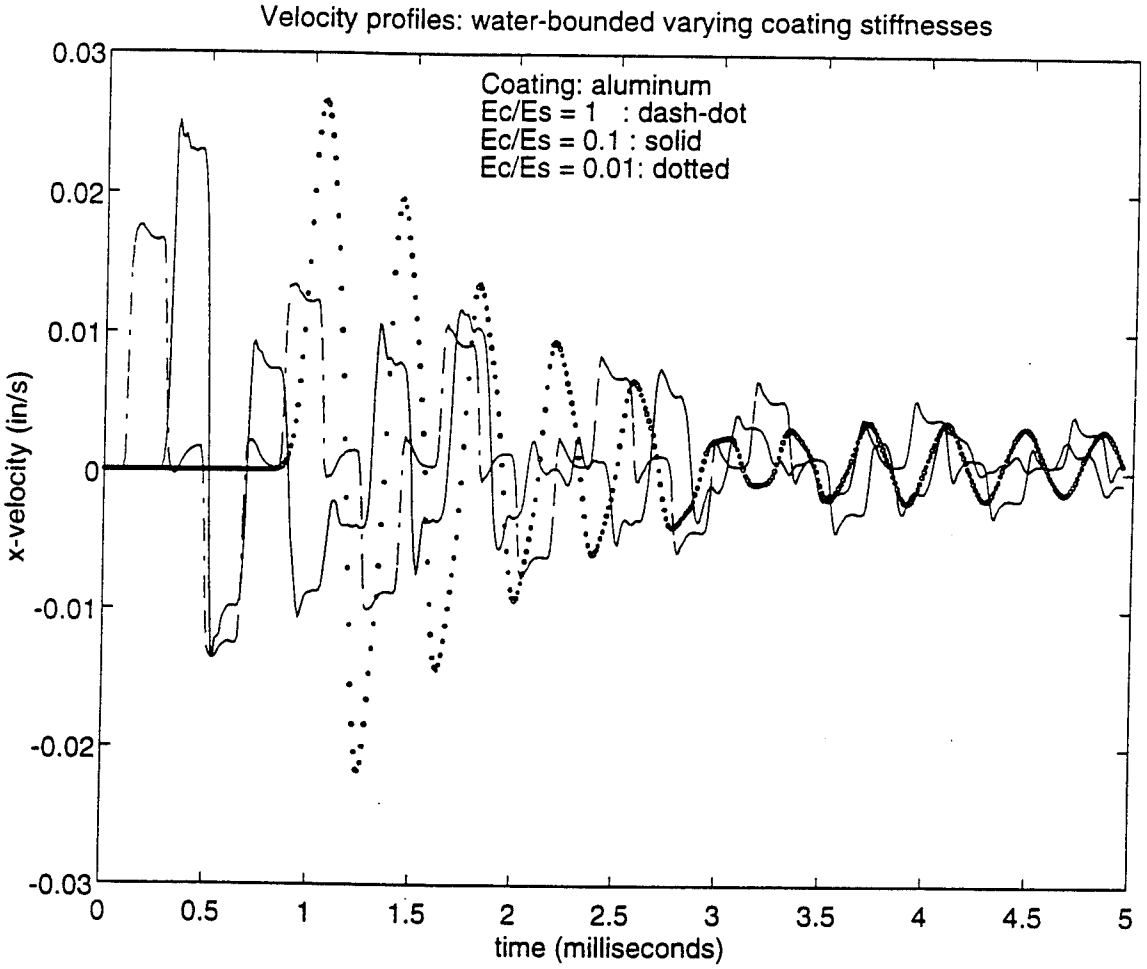

Figure 27. Comparing velocity profiles at a point near the interface on the structure for water-bounded systems with less stiff aluminum coatings: homogeneous, $E_c/E_s = 0.1$, $E_c/E_s = 0.01$

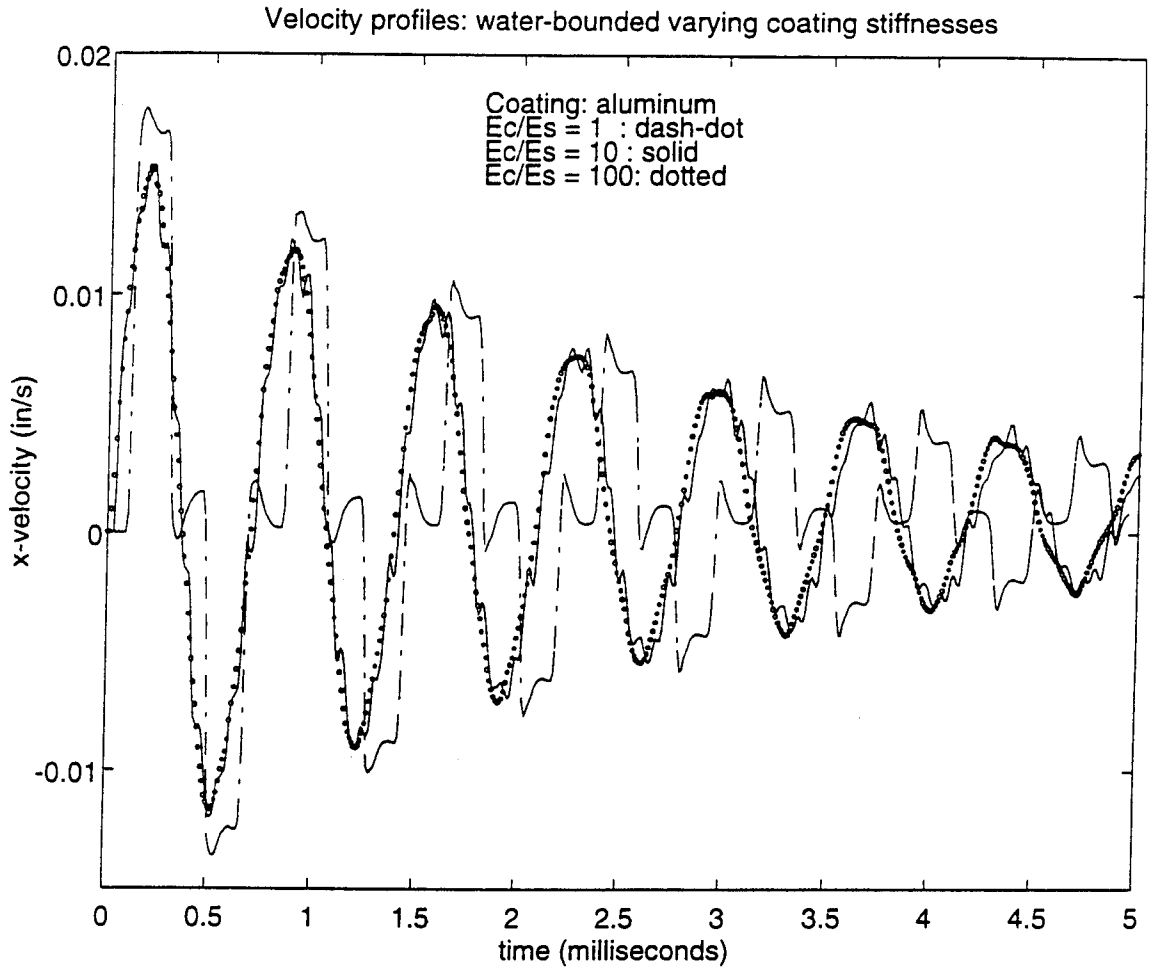

Figure 28. Comparing velocity profiles at a point near the interface on the structure for water-bounded systems with stiffer aluminum coatings: homogeneous, $E_c/E_s = 10$, $E_c/E_s = 100$

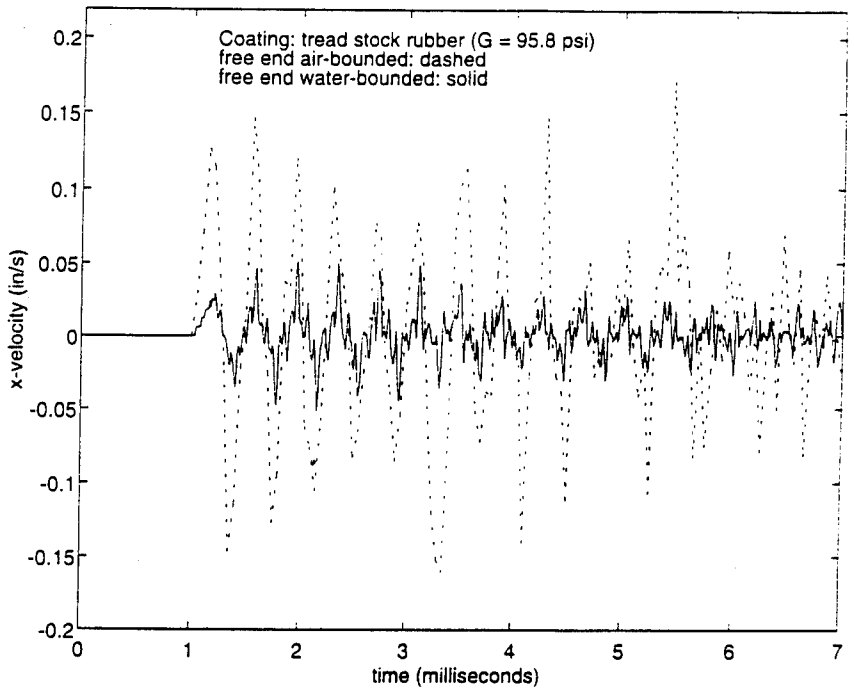

Figure 29. Comparing velocity profiles at a point near interface on structure for air-bounded vs. water-bounded systems with tread stock rubber (G = 95.8 psi) coating

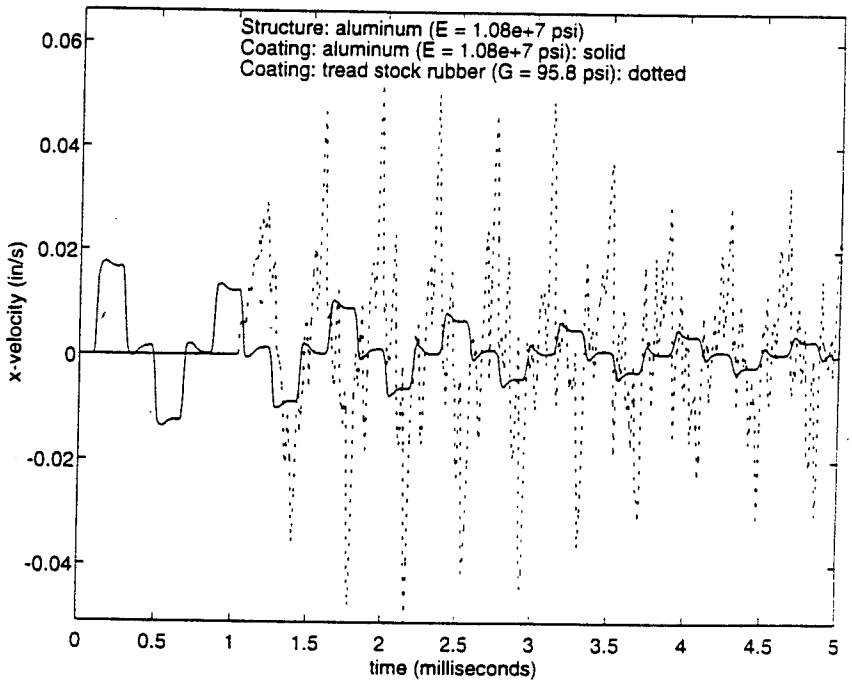

Figure 30. Comparing velocity profiles at a point near interface on structure for water-bounded aluminum versus tread stock rubber coated (G = 95.8 psi) systems

homogeneous system response (Figure 31). A more favorable dynamic response results when the rubber shear modulus is increased by a factor of 100; the nodal velocity is smaller than the nodal velocity of the homogeneous system (Figure 32).

Like the air-bounded model, a threshold coating value for a one-dimensional, water-bounded system exists at a rubber shear modulus between 958 psi and 9580 psi. Further investigation reveals that a shear modulus of 6000 psi and greater will result in a more favorable dynamic response (Figure 33).

The nodal velocity of a point in the structure increases with a decrease in the rubber impedance regardless of the bounding medium. The softer coating serves to trap the stress wave energy within the structure preventing energy dissipation from the structure to the water. This effect raises the overall stress state of the underlying structure closer to yield stress limits.

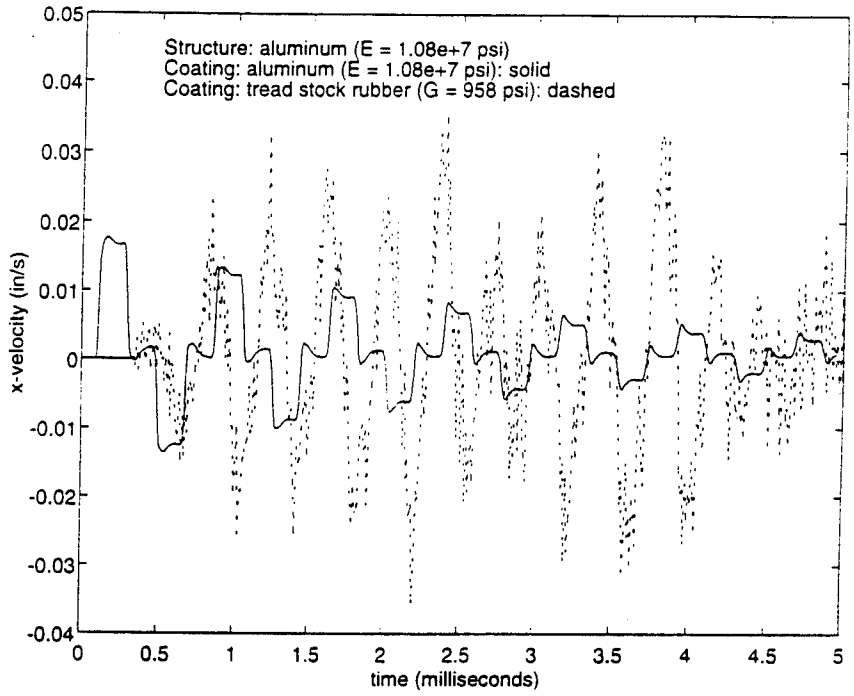

Figure 31. Comparing velocity profiles at a point near interface on structure for water-bounded aluminum versus stiffer tread stock rubber (G = 958 psi) coating

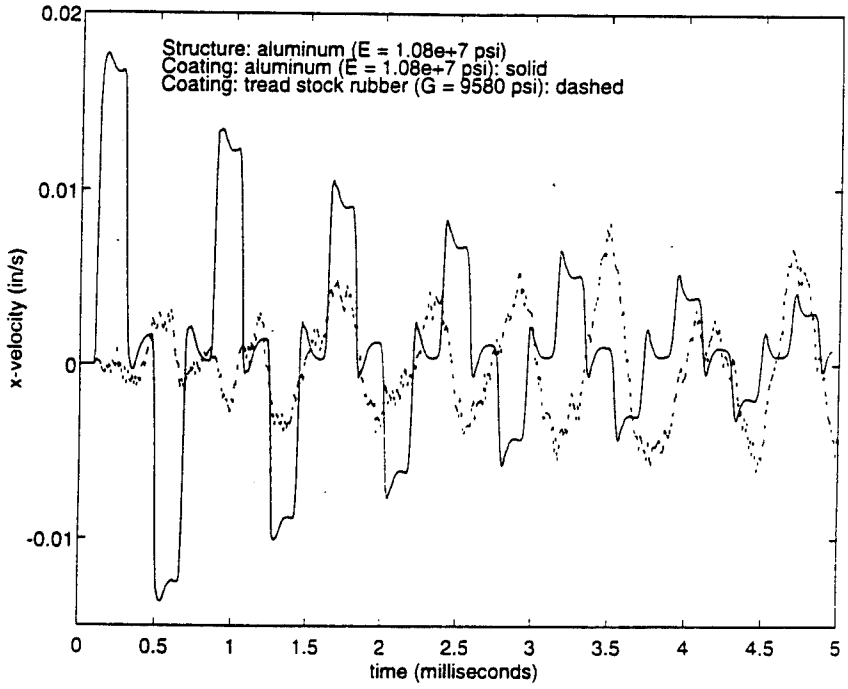

Figure 32. Comparing velocity profiles at a point near interface on structure for water-bounded aluminum versus stiffer tread stock rubber (G = 9580 psi) coating

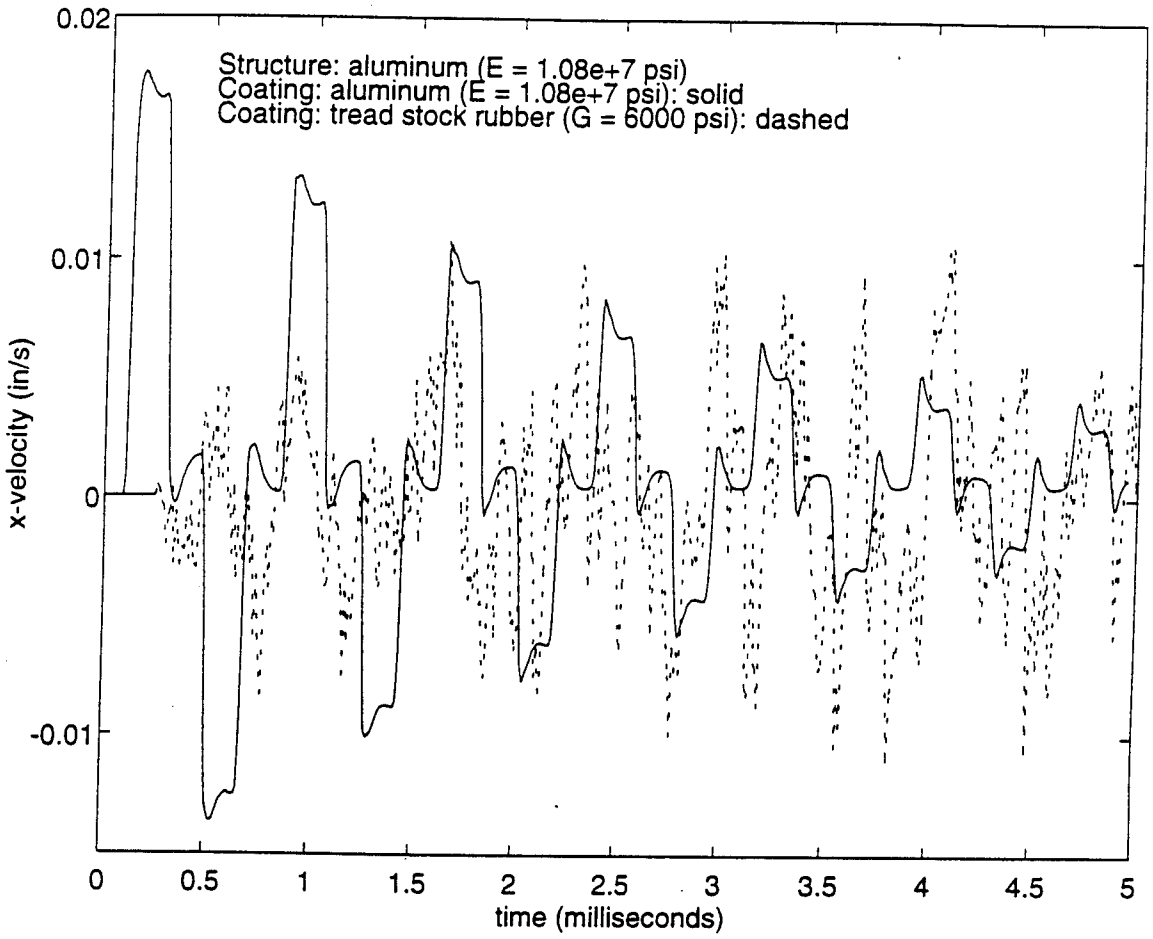

Figure 33. Comparing velocity profiles at a point near interface on structure for water-bounded aluminum versus tread stock rubber (G = 6000 psi) coating

V. ANALYSIS OF TWO-DIMENSIONAL MODEL

Data is collected at three distinct locations along the aluminum shell. Position "A" is the element where the underwater shock wave first impacts the structure, position "B" is an element on the bottom of the cylinder, and position "C" corresponds to the element furthest from the point of initial impact (Figure 34). The hoop and axial microstrains are reported at positions "A", "B", and "C".

A. ELEMENT COMPATIBILITY

Three computational models were used to represent an aluminum infinite cylinder as follows: single thickshell, double thickshell, and brick-thickshell elements. The thickshell element configuration is optimum for elastic materials such as aluminum or steel. Brick elements are needed to properly model nearly incompressible materials using VEC/DYNA3D. However, in order to combine two different types of elements, compatibility between them must be ascertained.

Comparison of the hoop and axial strains at "A", "B", and "C" on the cylinder shows that there is essentially no difference in the dynamic response between the three models (Figure 35 to Figure 40). Thus there is no interface problem between thickshell and brick elements. All subsequent models in this study will use brick elements for the coating and thickshell elements for the underlying structure.

B. INFINITE CYLINDER SUBJECTED TO PRESSURE WAVE

1. Elastic Versus Nearly Incompressible Rubber Coating

With element compatibility established, the parametric study is now extended to the response of a two-dimensional, infinite cylinder subjected to an underwater unit step pressure wave.

First, the response of an uncoated aluminum cylinder will be compared to two coated models. An elastic-coated model uses

two-dimensional model

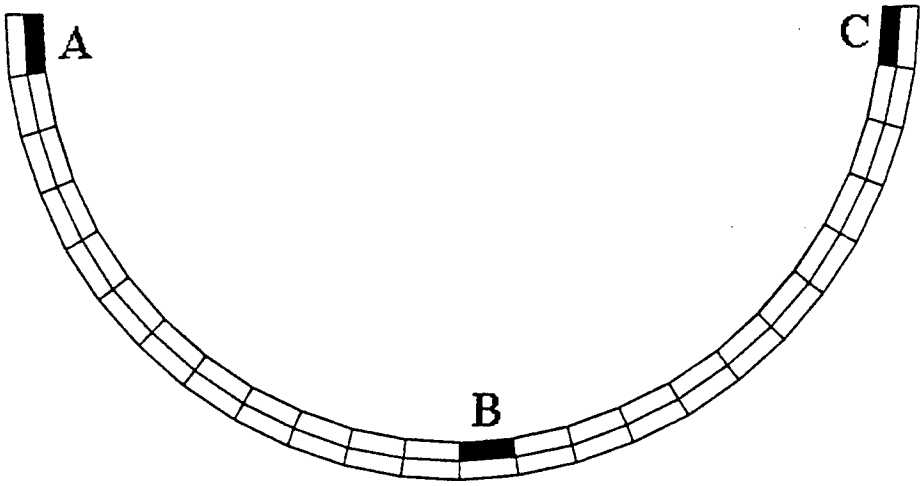

inner ring: aluminum shell
outer ring: cylindrical coating

Figure 34. Locations along aluminum structure used for data recording (Positions A, B, and C)

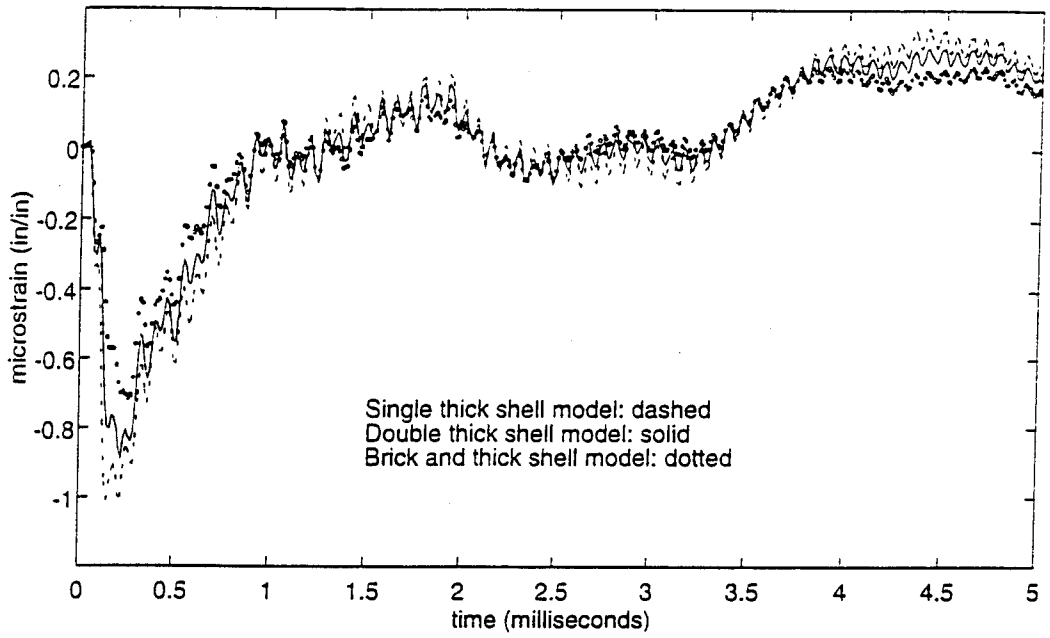

Figure 35. Hoop strain at position A for different element configurations

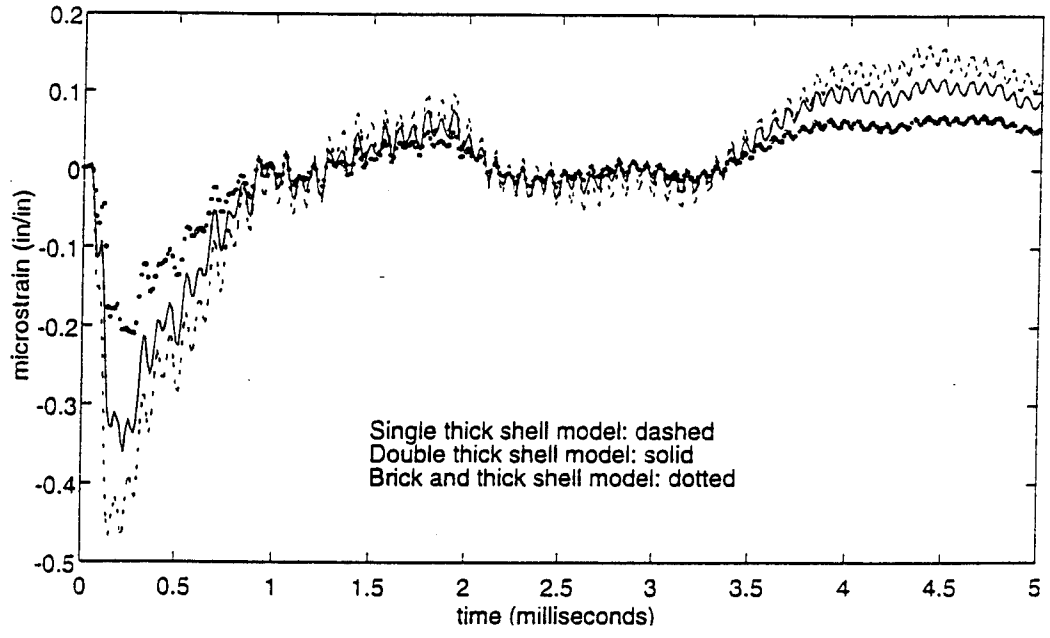

Figure 36. Axial strain at position A for different element configurations

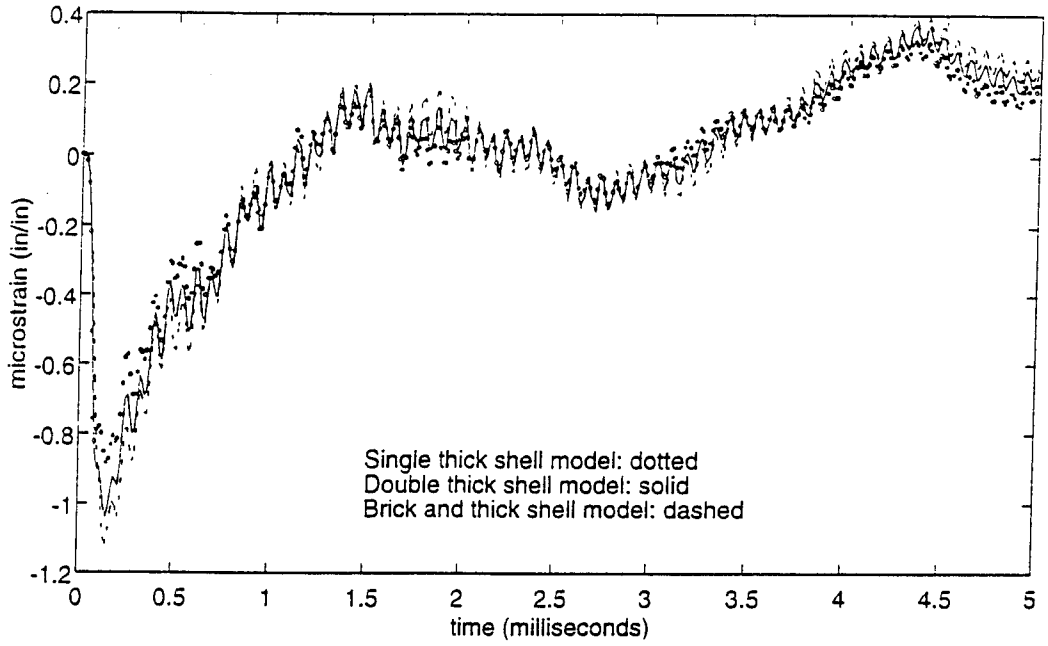

Figure 37. Hoop strain at position B for different element configurations

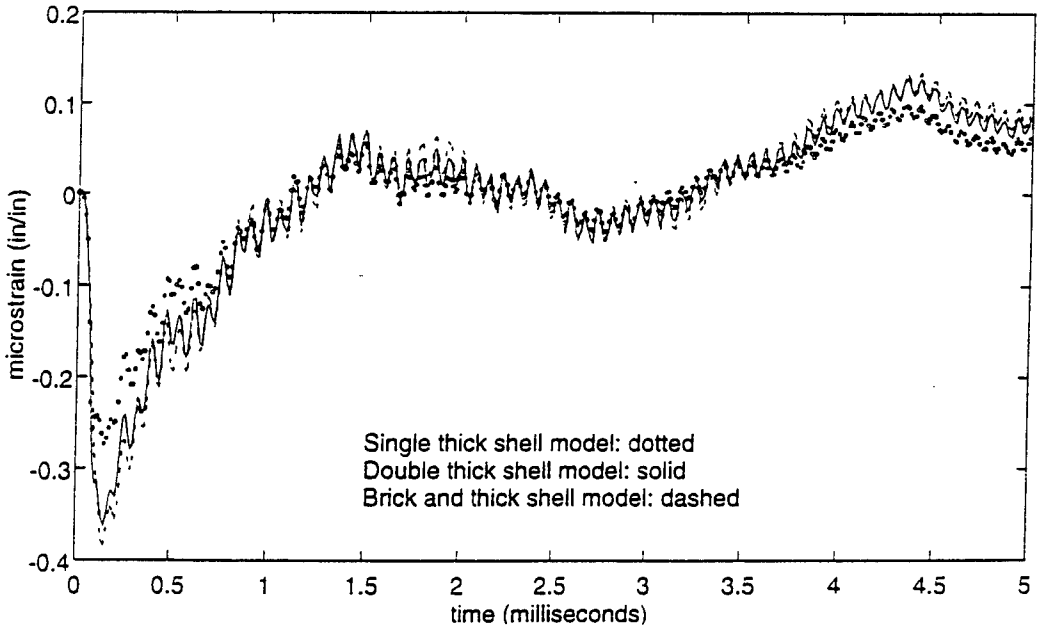

Figure 38. Axial strain at position B for different element configurations

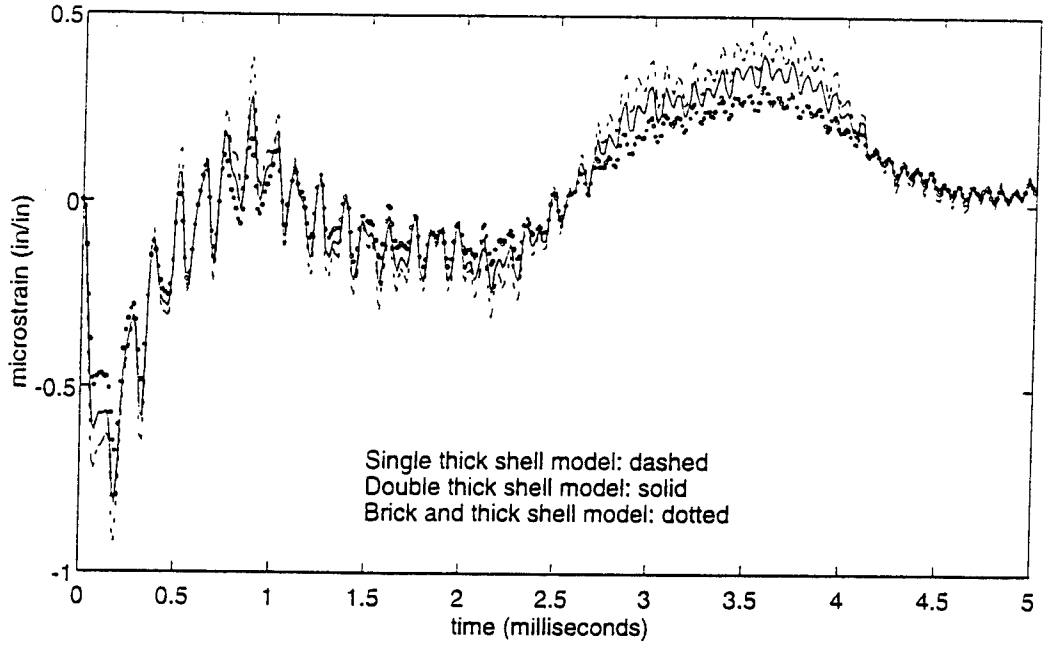

Figure 39. Hoop strain at position C for different element configurations

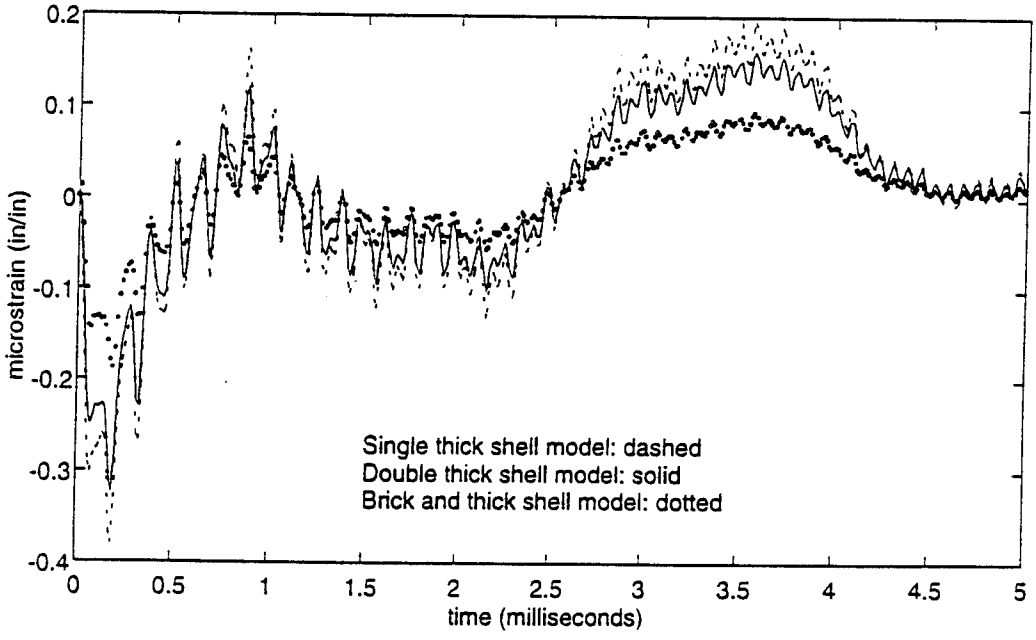

Figure 40. Axial strain at position C for different element configurations

aluminum with an identical impedance value for both the coating and structure (i.e., $E_c/E_s = 1$). A rubber-coated model uses tread stock rubber with a shear modulus of 95.8 psi. The coating and structure are each one-quarter inch thick.

The strains at positions "A", "B", and "C" are compared (Figure 41 to Figure 46). In all six cases, the rubber-coated shell exhibits significantly higher magnitudes of strain than the all-aluminum models. The nearly incompressible rubber coating maintains the underlying structure at a higher strain state for approximately 4 milliseconds after impact. Therefore, the internal energy of the aluminum shell will be higher (Figure 47).

2. Effect of Rubber Coating Impedance

In the one-dimensional system analysis, a threshold value for the rubber shear modulus was obtained for the given system configuration. Moreover, this procedure can be applied to a two-dimensional system with the coating and structure both equal to 0.25 inches. Consider the case where the shear modulus and coating impedance of the tread stock rubber is altered by a factor of five and ten to 500 psi and 1000 psi, respectively. These coated models are compared to an uncoated shell.

There is a distinct difference in the strain magnitudes between the three cases at each location along the structure (Figure 48 to Figure 53). The threshold value for a rubber shear modulus exists between 500 psi and 1000 psi by comparing the strain magnitudes of the three models. As previously described, the threshold value is case dependent. There is a significant difference in the threshold values comparing the one-dimensional system to the infinite cylinder. The results show an increase in the fixed difference between the rubber coating and elastic shell impedances for the infinite cylinder.

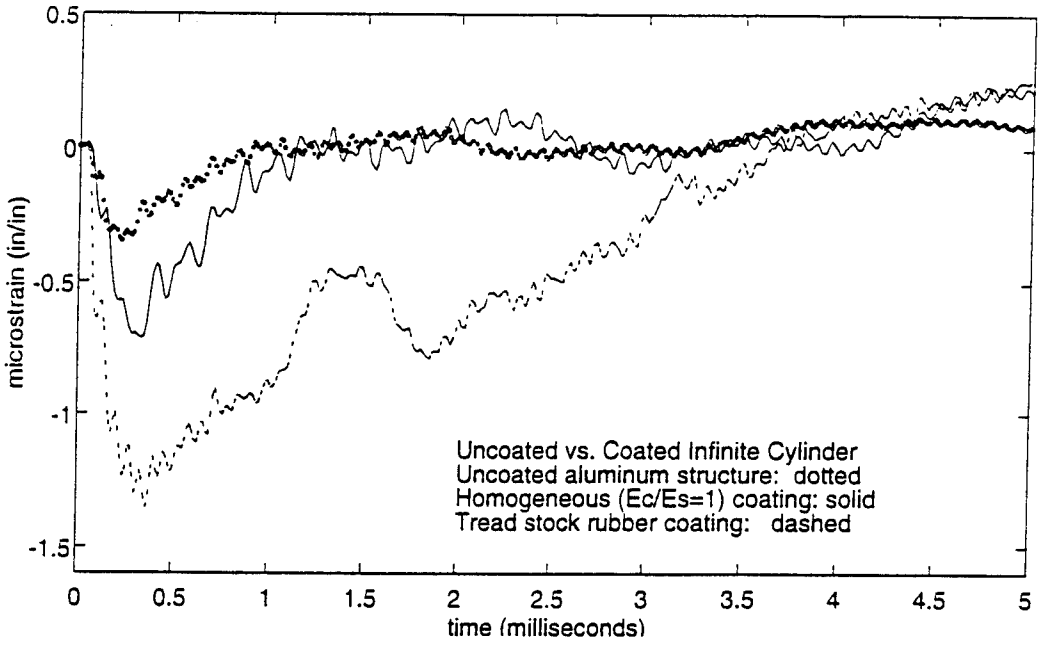

Figure 41. Hoop strain at position A for uncoated and coated aluminum cylinders

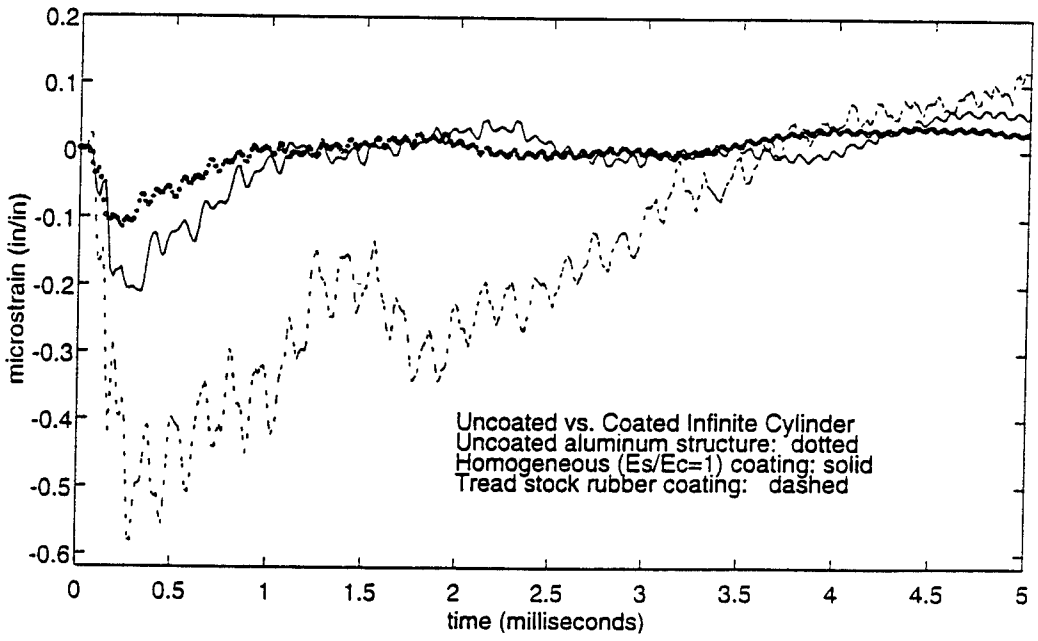

Figure 42. Axial strain at position A for uncoated and coated aluminum cylinders

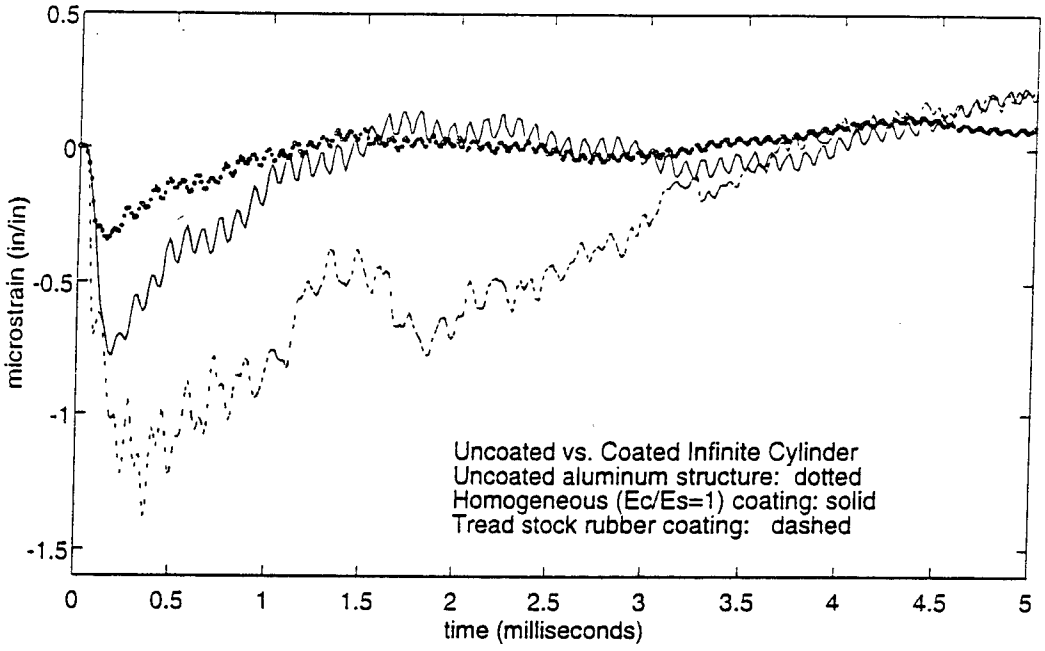

Figure 43. Hoop strain at position B for uncoated and coated aluminum cylinders

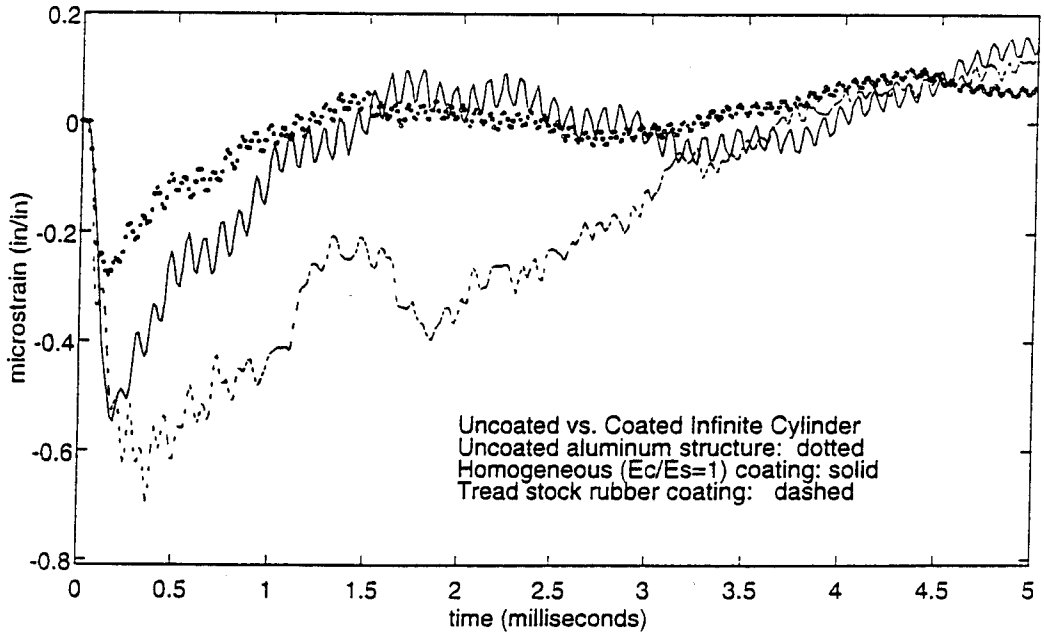

Figure 44. Axial strain at position B for uncoated and coated aluminum cylinders

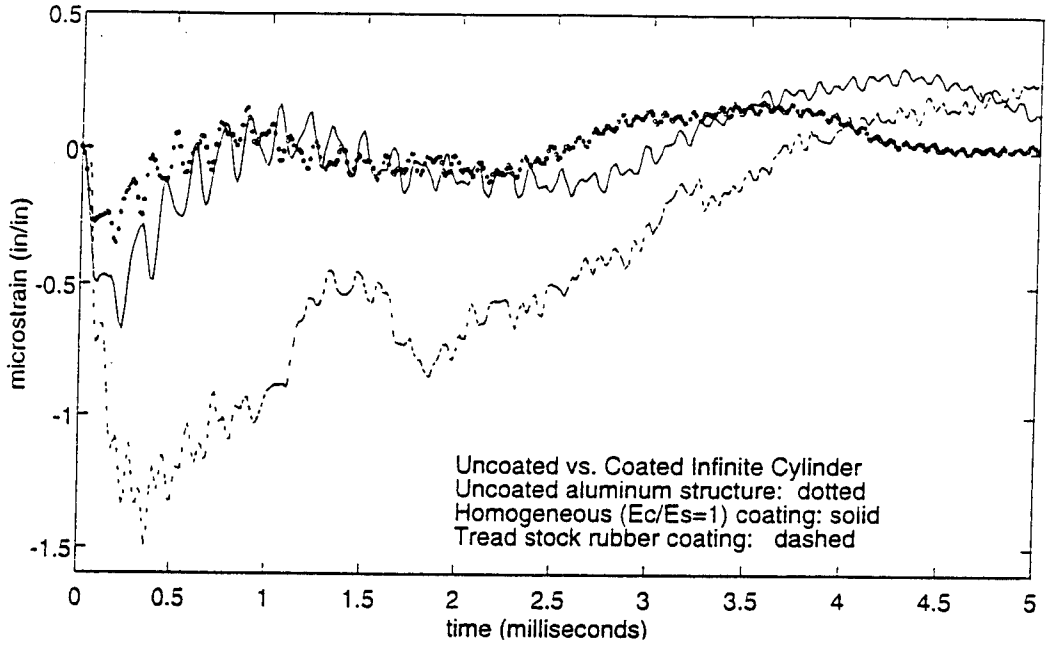

Figure 45. Hoop strain at position C for uncoated and coated aluminum cylinders

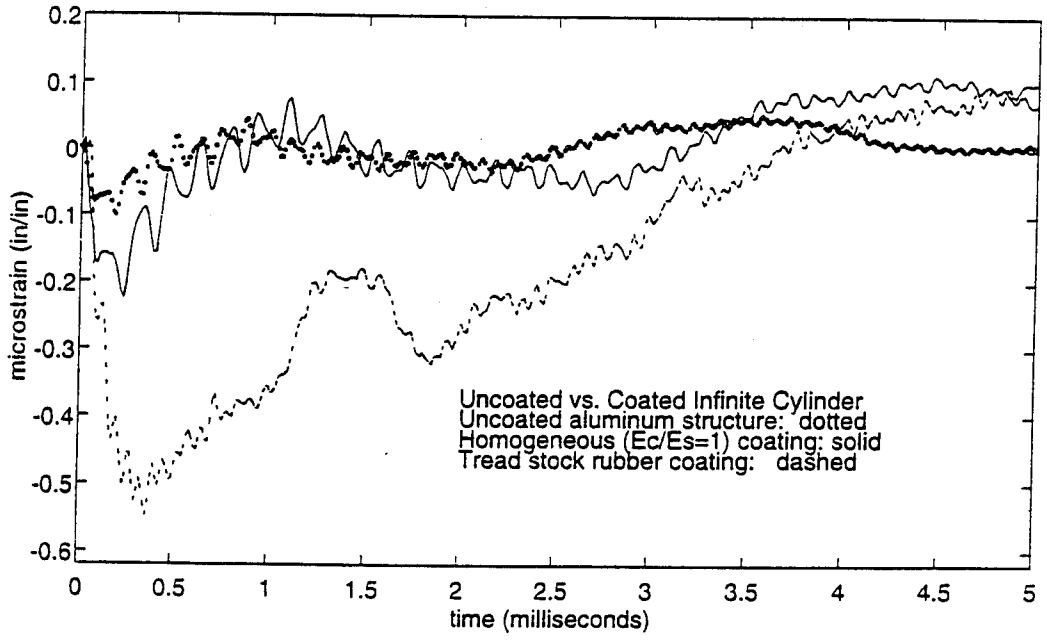

Figure 46. Axial strain at position C for uncoated and coated aluminum cylinders

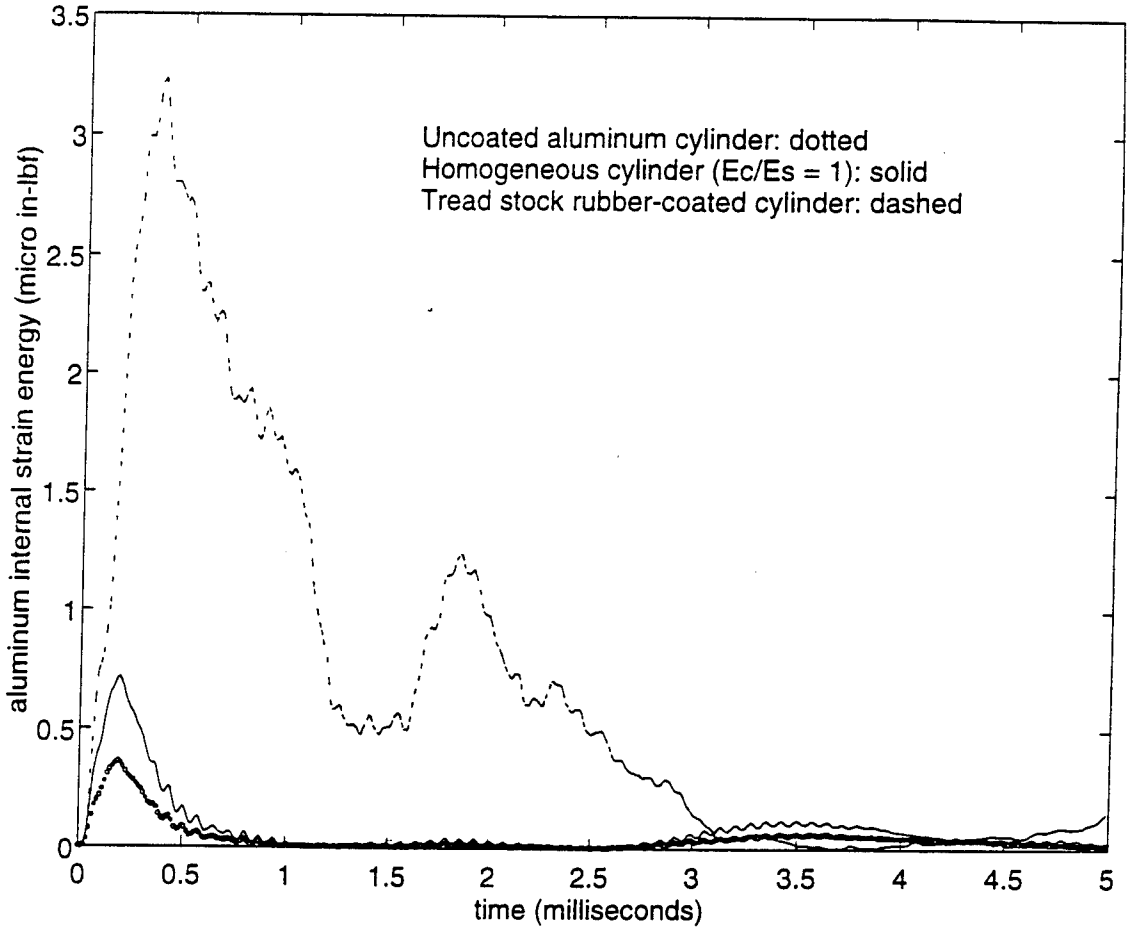

Figure 47. Comparing internal energy of aluminum shell using cylinders with no coating, elastic coating, and rubber coating

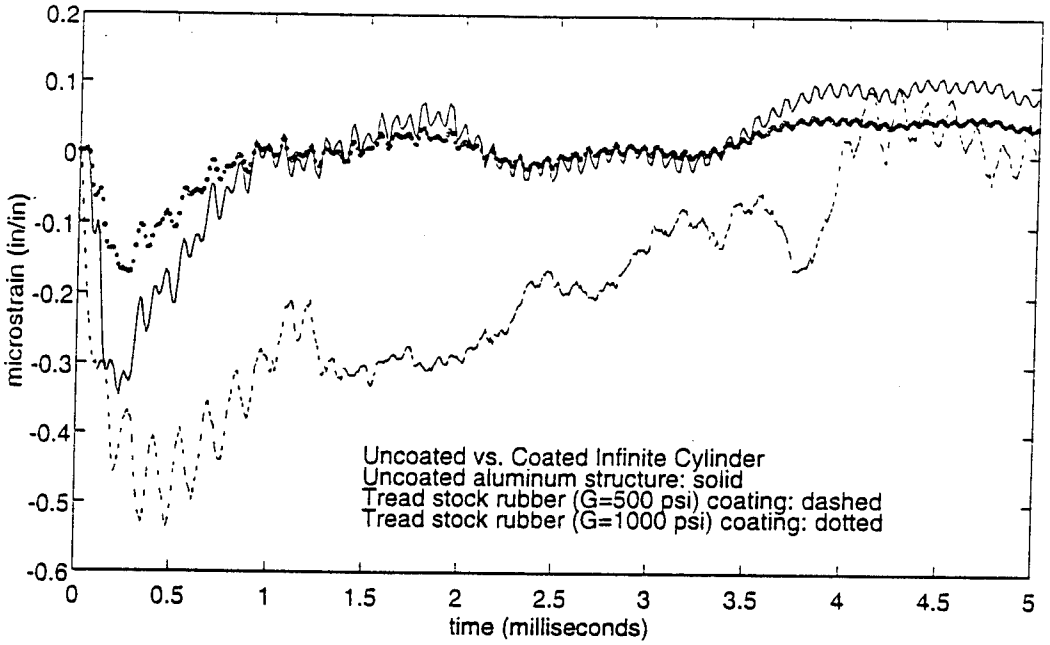

Figure 48. Hoop strain at position A for rubber-coated aluminum cylinders with varying shear moduli

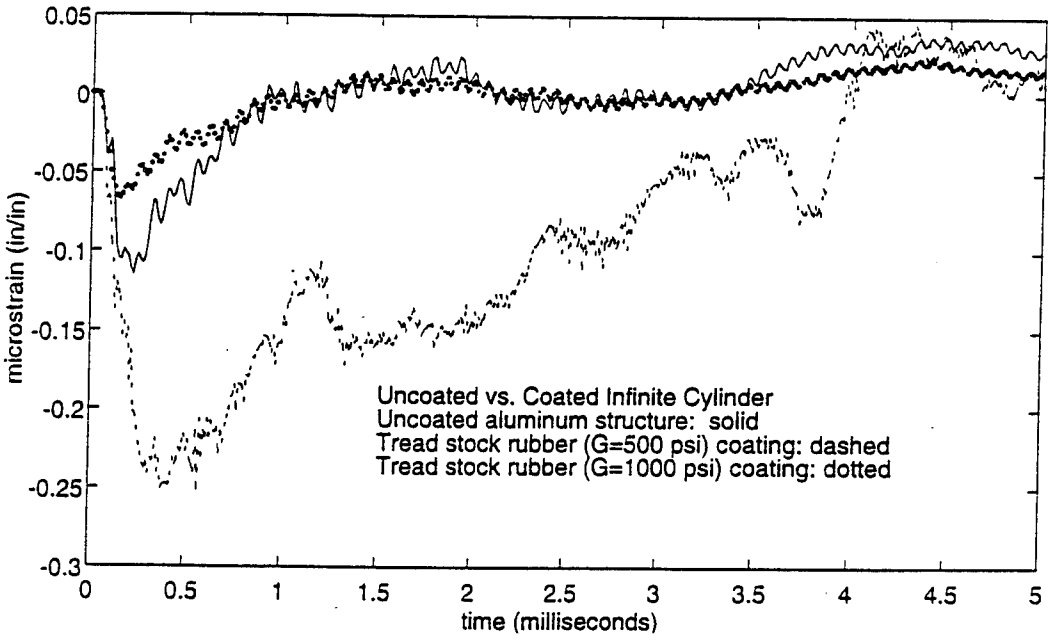

Figure 49. Axial strain at position A for rubber-coated aluminum cylinders with varying shear moduli

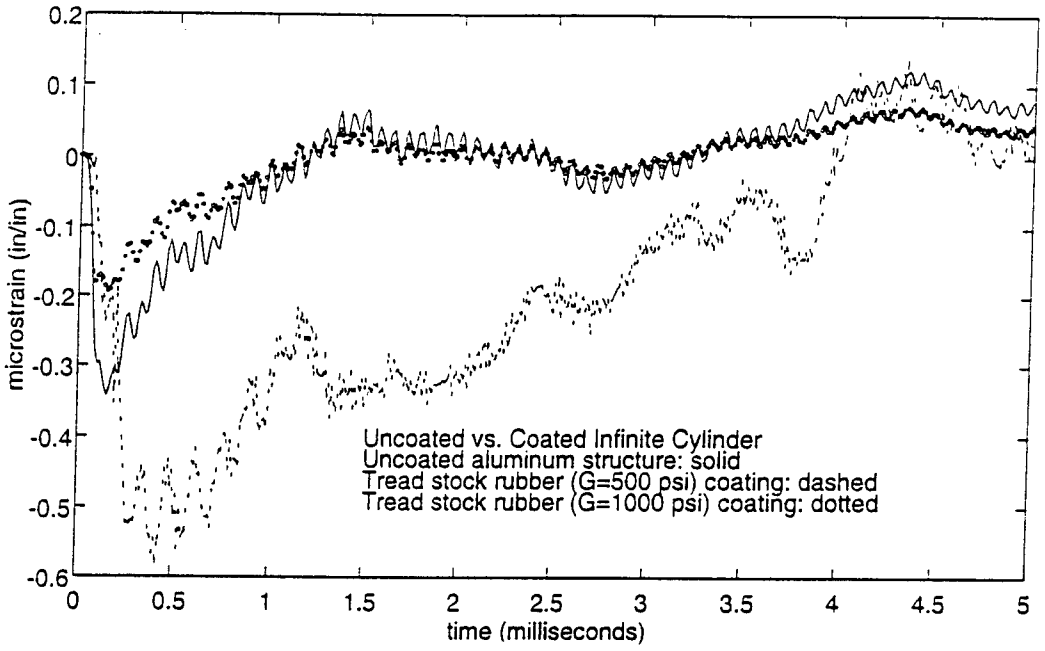

Figure 50. Hoop strain at position B for rubber-coated aluminum cylinders with varying shear moduli

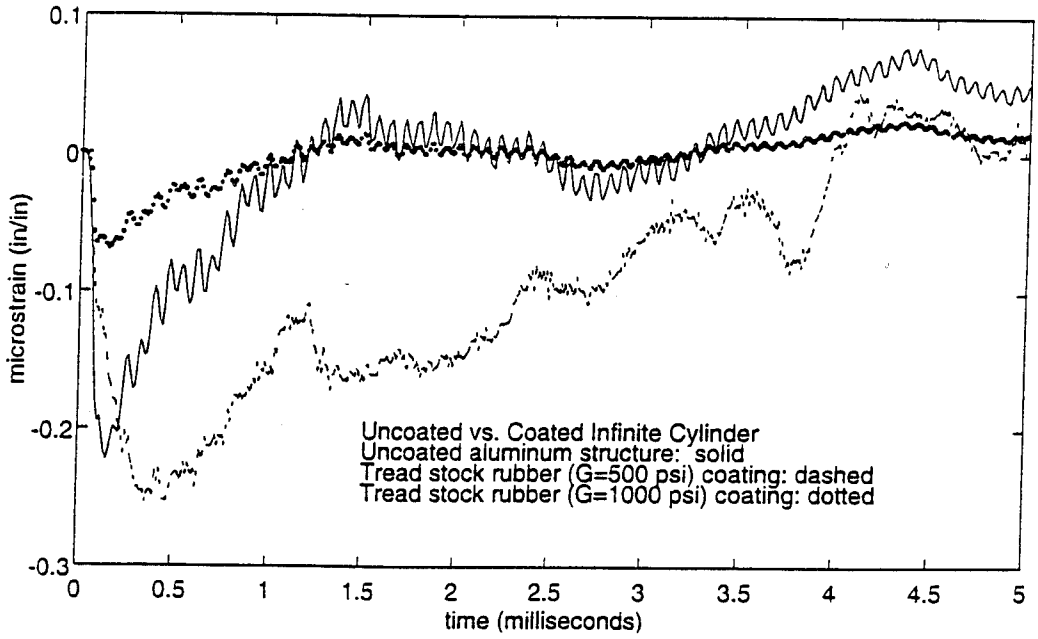

Figure 51. Axial strain at position B for rubber-coated aluminum cylinders with varying shear moduli

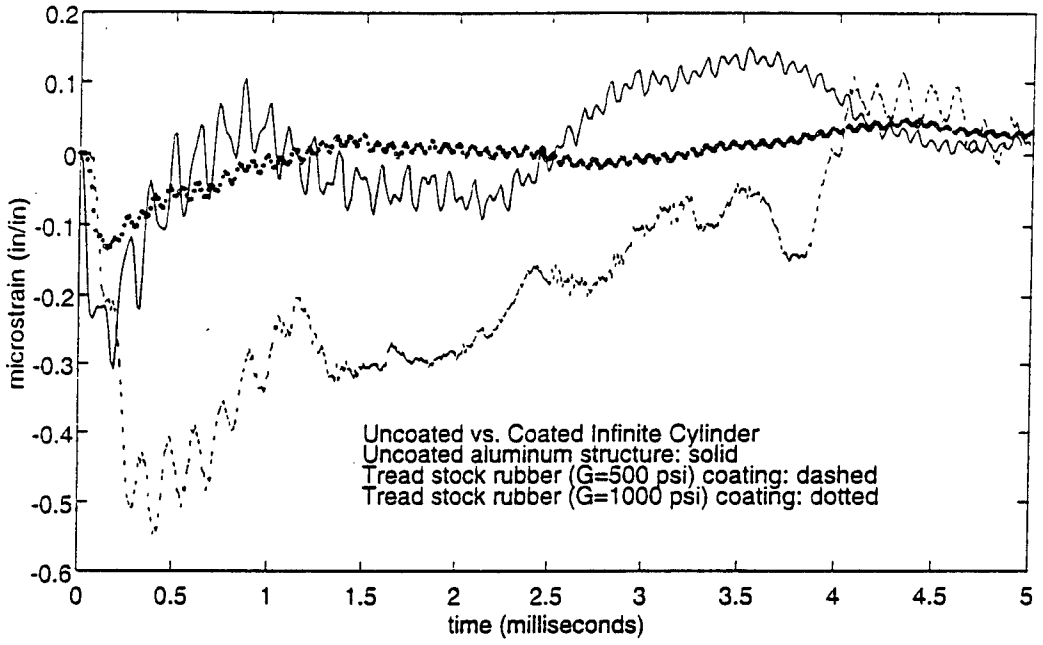

Figure 52. Hoop strain at position C for rubber-coated aluminum cylinders with varying shear moduli

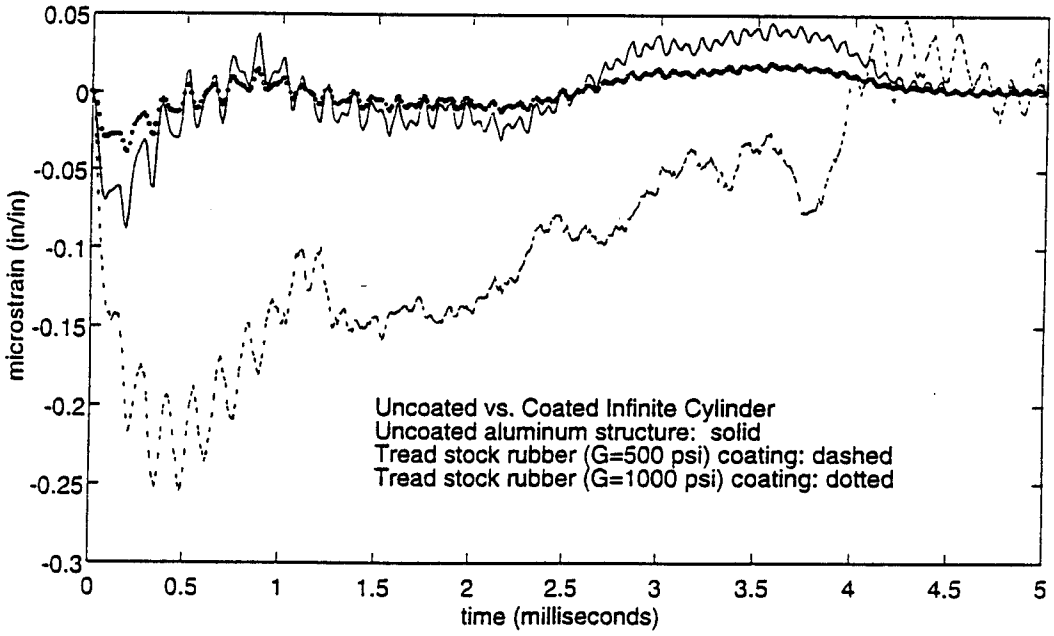

Figure 53. Axial strain at position C for rubber-coated aluminum cylinders with varying shear moduli

The dynamic response of the cylinder in each case is dependent upon traverse time of the elastic wave through the coating. As in the one-dimensional case, the softer rubber coating induced a greater magnitude of strain in the underlying structure. Conversely, the larger shear modulus reduces the strain magnitude of the elastic shell and permits a greater amount of strain wave energy to be transferred to the coating from the structure where more energy can then be dissipated to the surrounding water medium (Figure 54). This observation is consistent regardless of the type and location of strain recorded.

A larger coating impedance is characterized by a larger shear modulus, which implies a stiffer coating material. A stiffer rubber coating consistently evokes a favorable response over the dynamic response of the uncoated cylinder subjected to identical shock conditions. Consider an alternative to varying the coating stiffness which involves changing the thickness of the rubber coating while holding the shear modulus constant. The dynamic response of aluminum cylinders coated with 0.125, 0.250, and 0.500 inch-thick tread stock rubber are compared in Figure 55 to Figure 60. The coating shear modulus is held constant at 95.8 psi.

The thicker rubber coating induced a smaller strain in the underlying structure as expected. This example does not involve altering the impedance of the rubber in terms of its material properties. However, the effect of increasing the thickness is analogous to increasing the shear modulus, which will increase the coating impedance. More energy is exchanged from the structure to the coating thereby lowering the structure's internal energy (Figure 61).

Since there is correlation between a stiffer coating and a thicker coating, it must follow that a threshold value exists in terms of a particular coating thickness or combination of stiffness and thickness. The above example

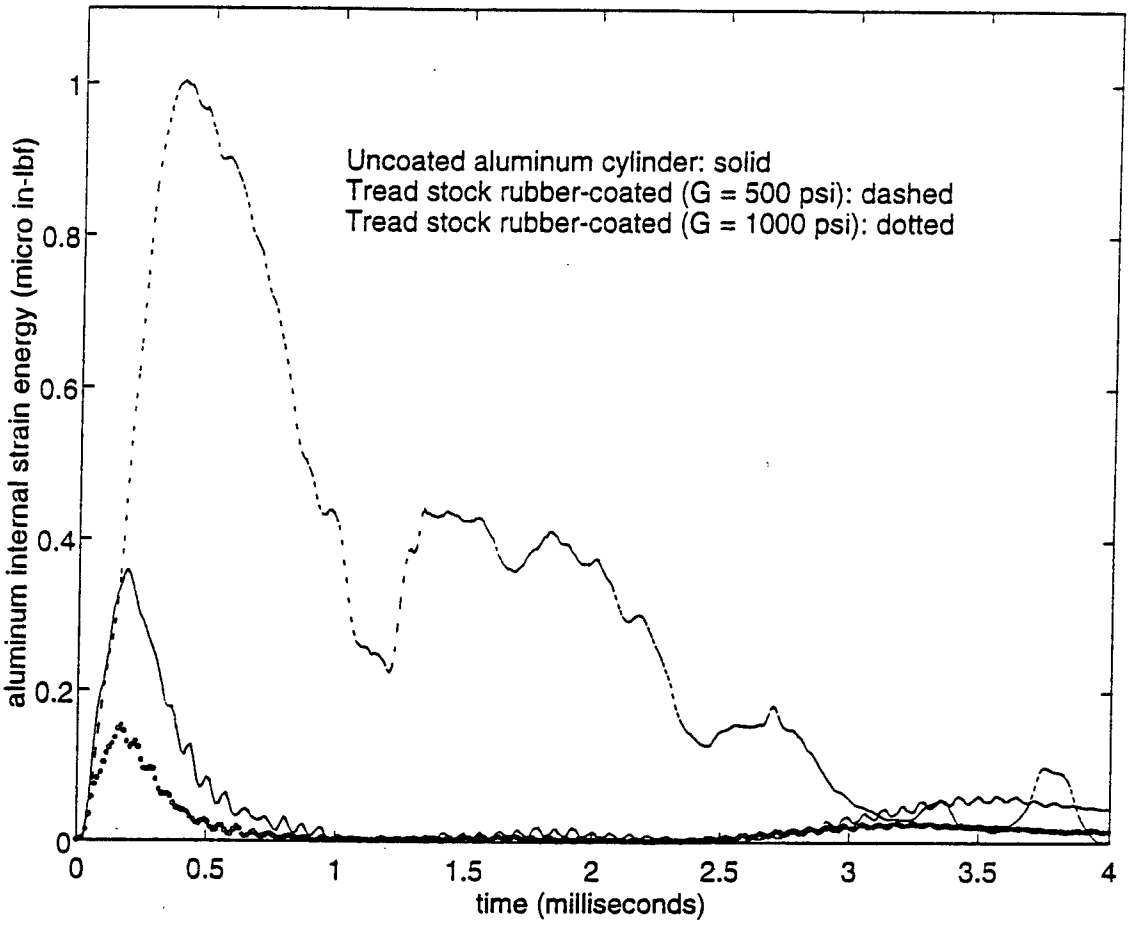

Figure 54. Comparing internal energy of aluminum shell for cylinders with rubber coating of variable shear moduli

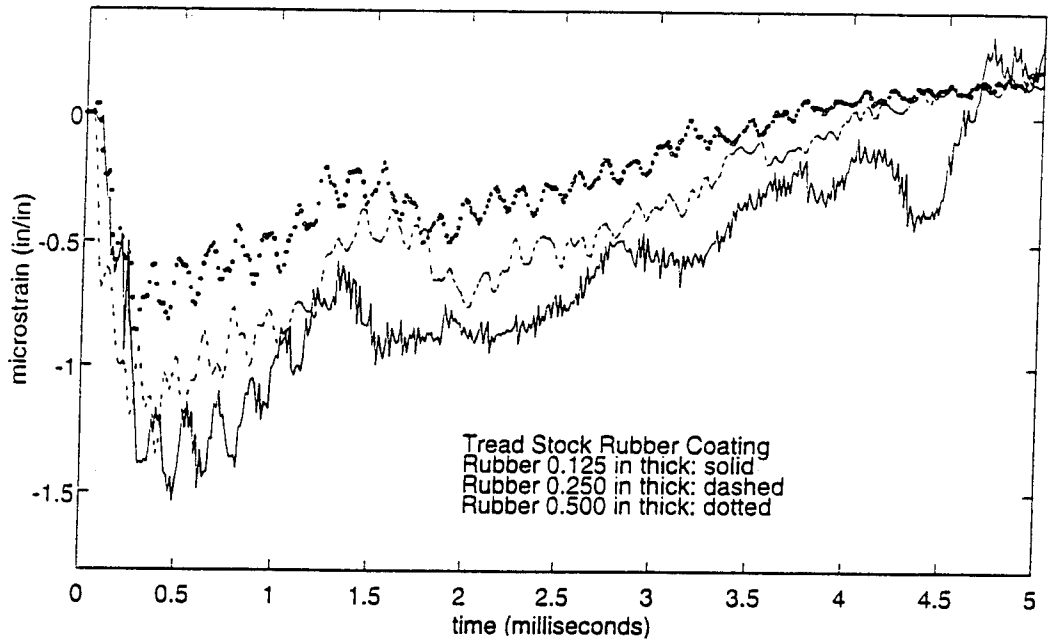

Figure 55. Hoop strain at position A for rubber-coated aluminum cylinders of varying coating thicknesses

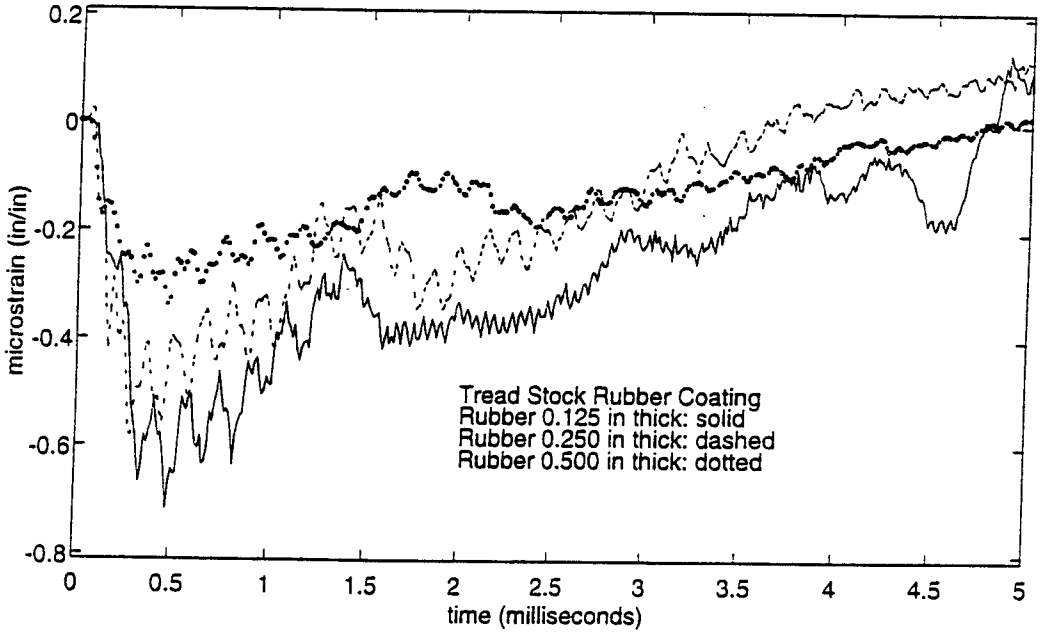

Figure 56. Axial strain at position A for rubber-coated aluminum cylinders of varying coating thicknesses

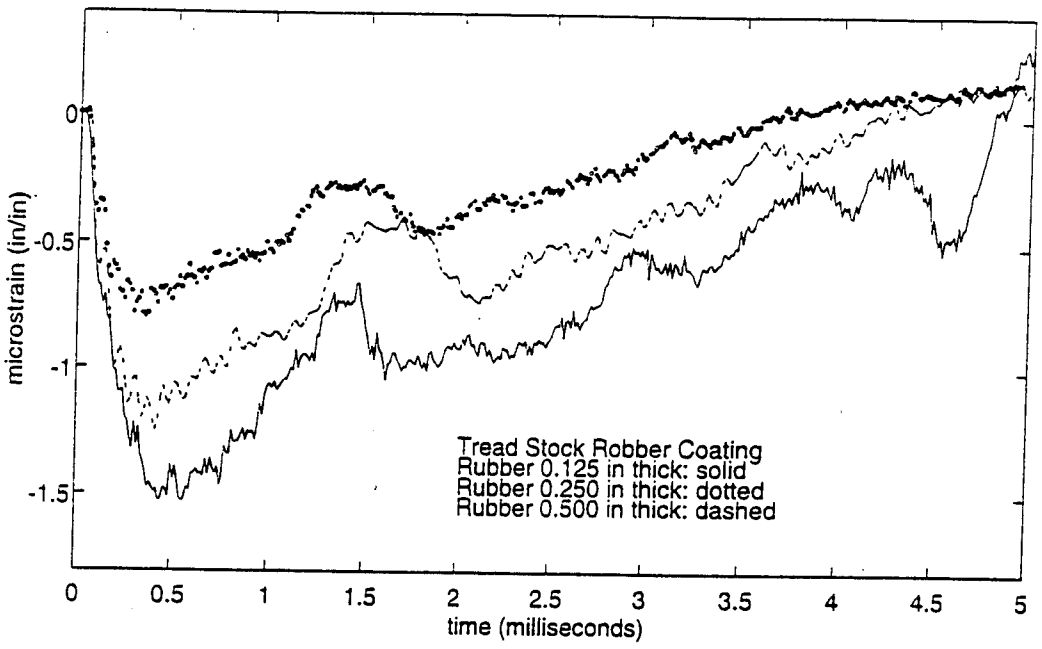

Figure 57. Hoop strain at position B for rubber-coated aluminum cylinders of varying coating thicknesses

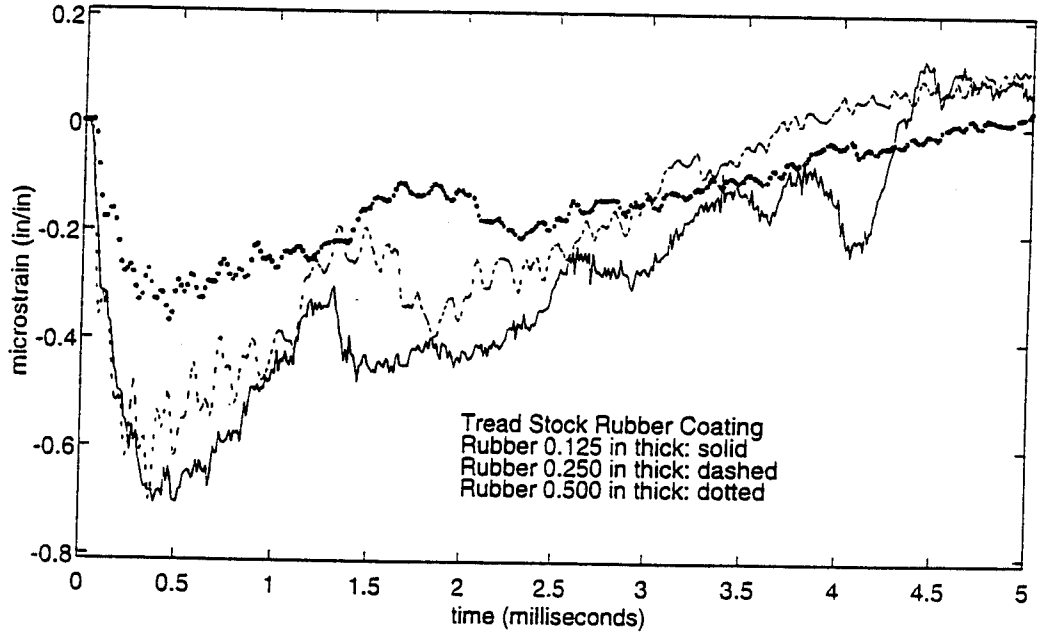

Figure 58. Axial strain at position B for rubber-coated aluminum cylinders of varying coating thicknesses

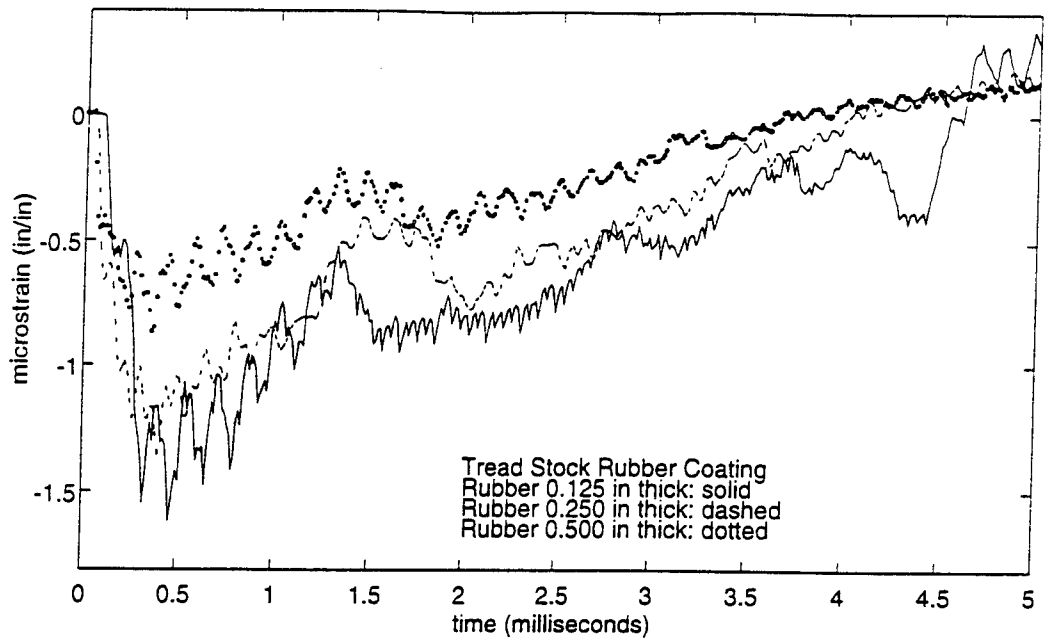

Figure 59. Hoop strain at position C for rubber-coated aluminum cylinders of varying coating thicknesses

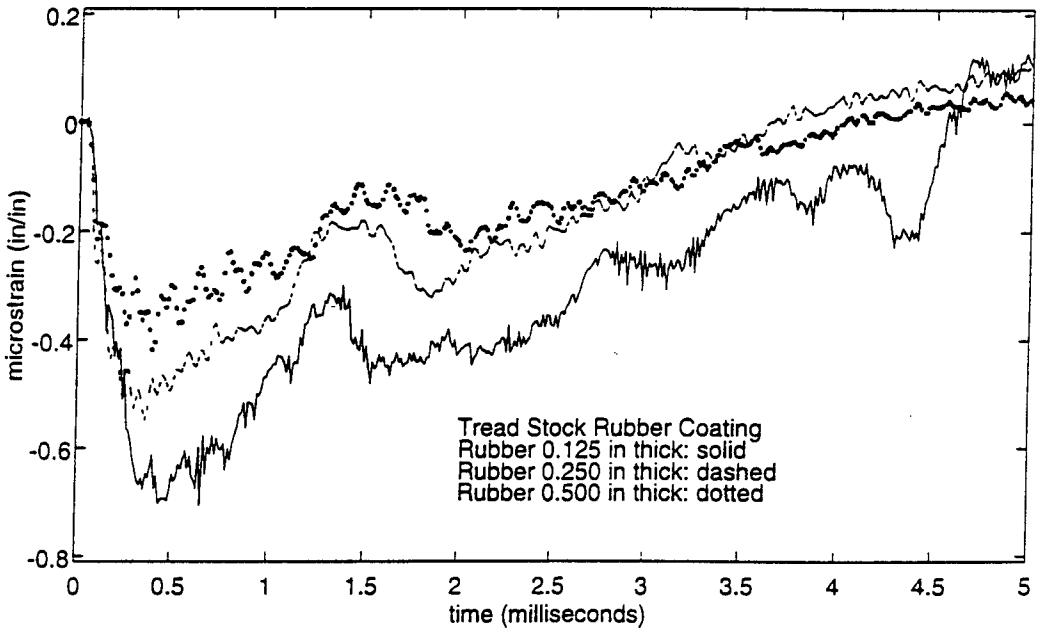

Figure 60. Axial strain at position C for rubber-coated aluminum cylinders of varying coating thicknesses

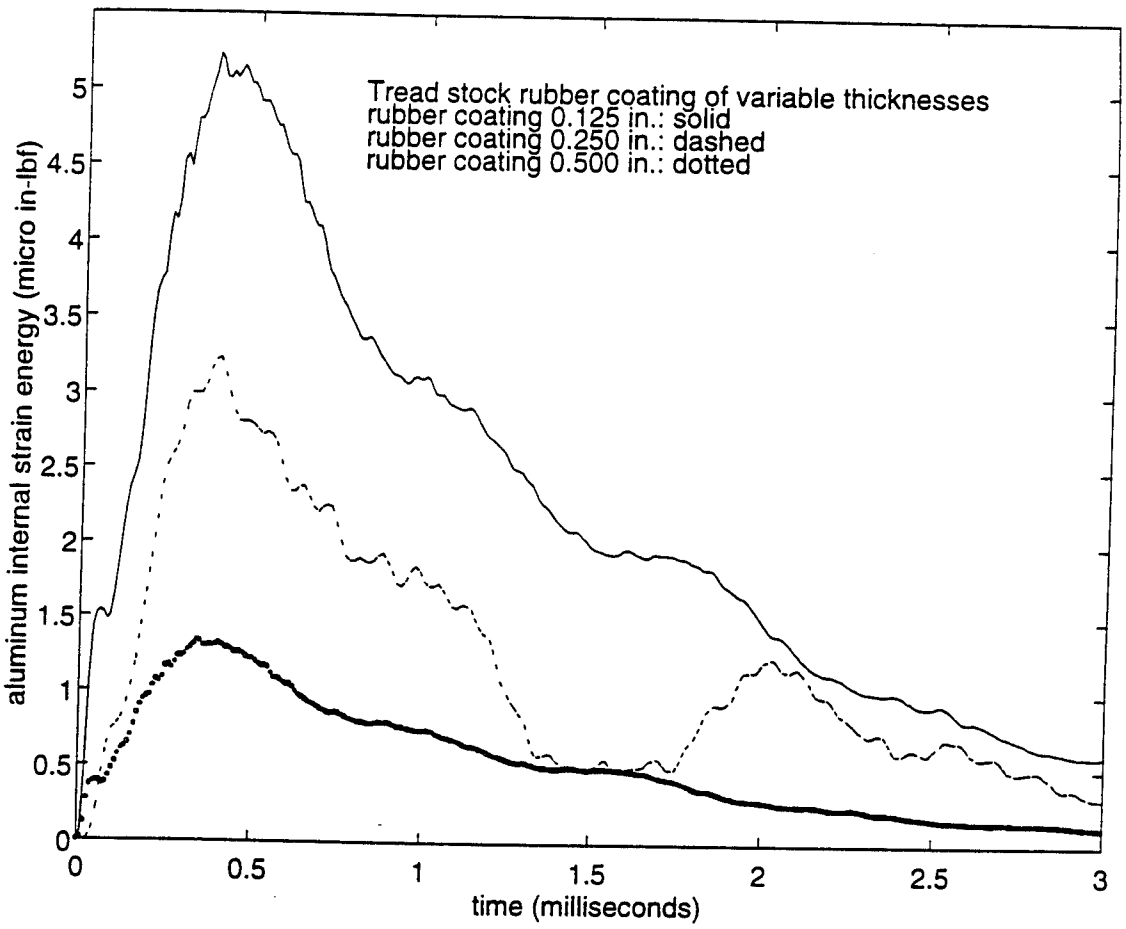

Figure 61. Comparing internal energy of aluminum shell with rubber coating of variable thicknesses

failed to prove the existence of a threshold value for thickness because all the strains observed were well above the strains of the uncoated shell. If the rubber shear modulus is increased by a factor of 5 to 500 psi, the strains induced in the shell at all three locations are presented in Figure 62 to Figure 67. The threshold value clearly exists at a coating thickness between 0.25 inch and 0.5 inch for the model with a constant shear modulus of 500 psi. The corresponding internal energy of the shell for each case is given in Figure 68. The values of shell internal energy are reduced at coating thicknesses greater than the threshold coating thickness value as expected.

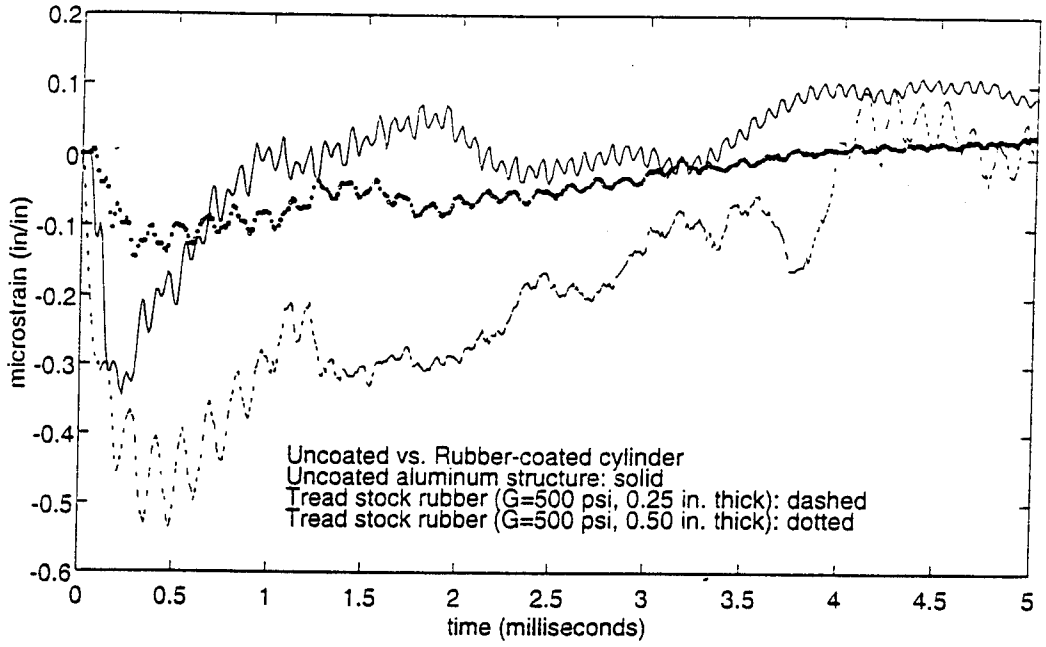

Figure 62. Hoop strain at position A for uncoated vs. coated aluminum cylinders of varying coating thicknesses and constant shear modulus of 500 psi

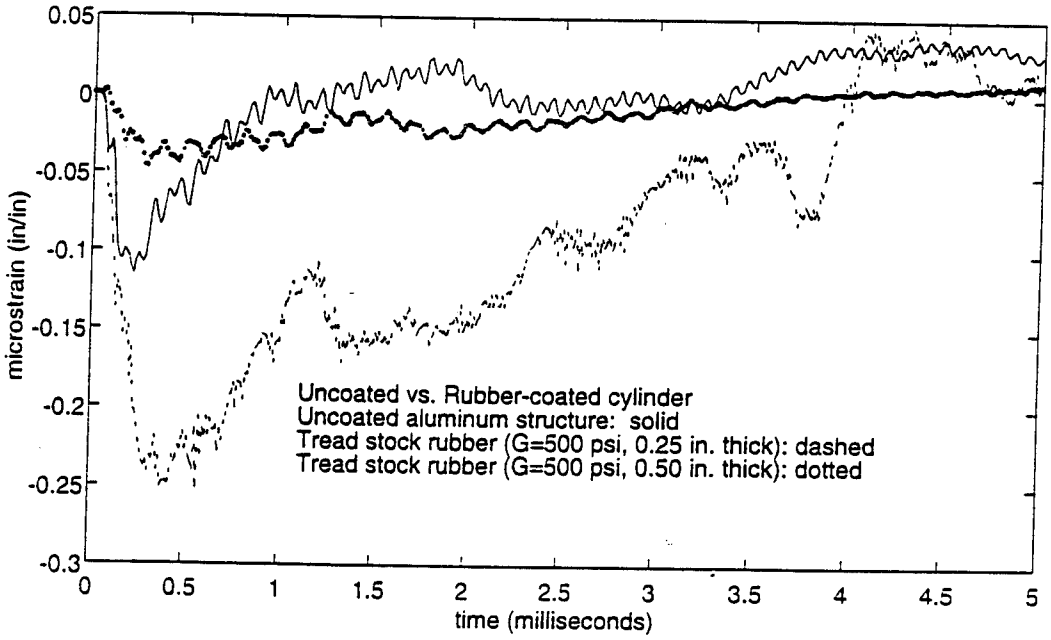

Figure 63. Axial strain at position A for uncoated vs. coated aluminum cylinders of varying coating thicknesses and constant shear modulus of 500 psi

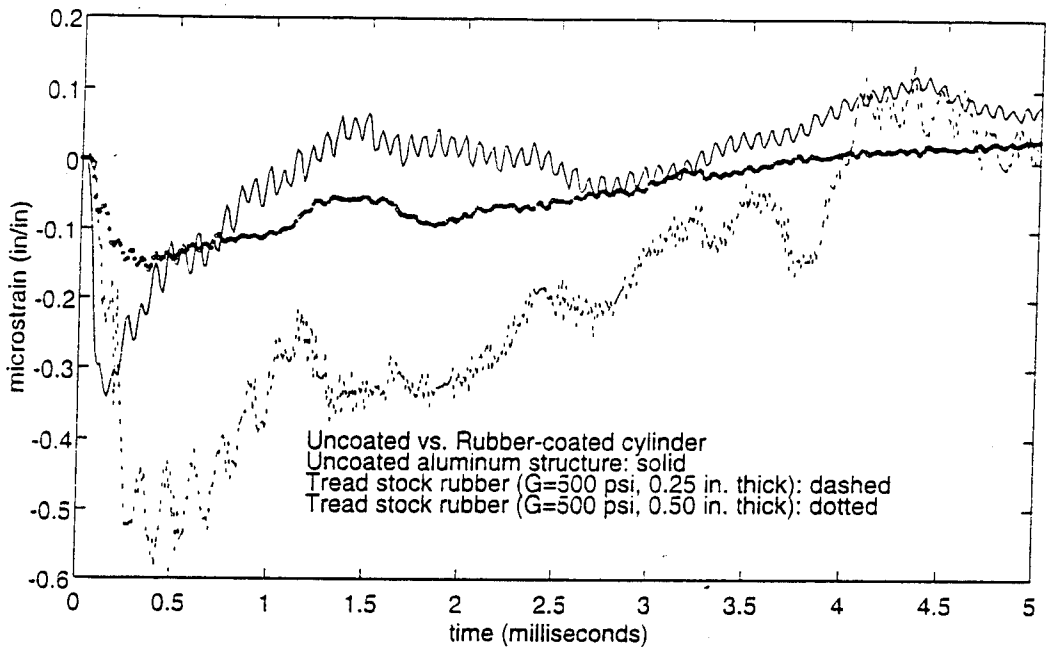

Figure 64. Hoop strain at position B for uncoated vs. coated aluminum cylinders of varying coating thicknesses and constant shear modulus of 500 psi

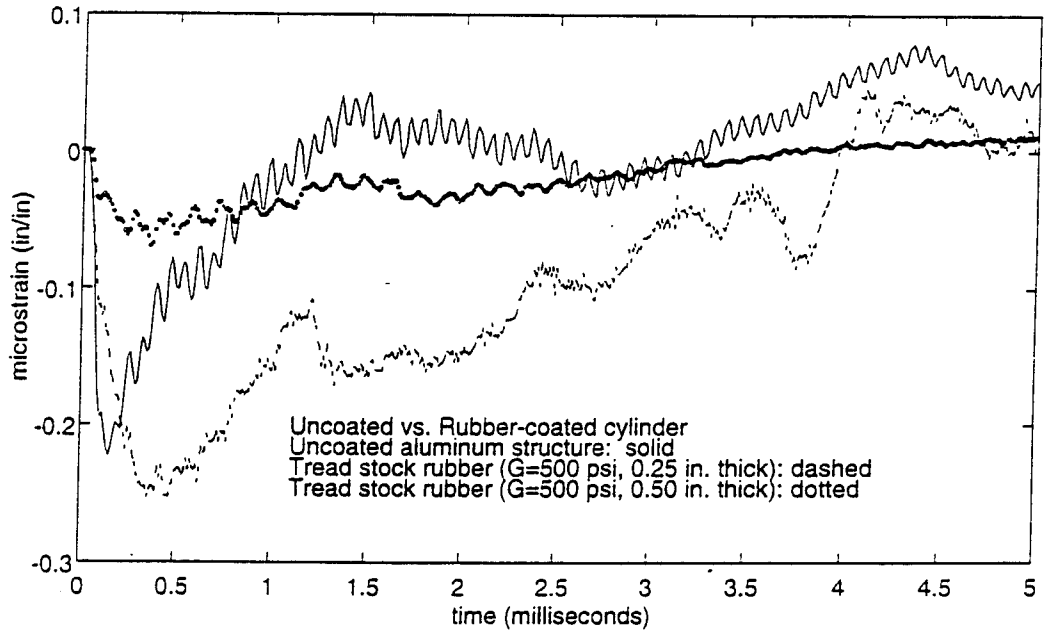

Figure 65. Axial strain at position B for uncoated vs. coated aluminum cylinders of varying coating thicknesses and constant shear modulus of 500 psi

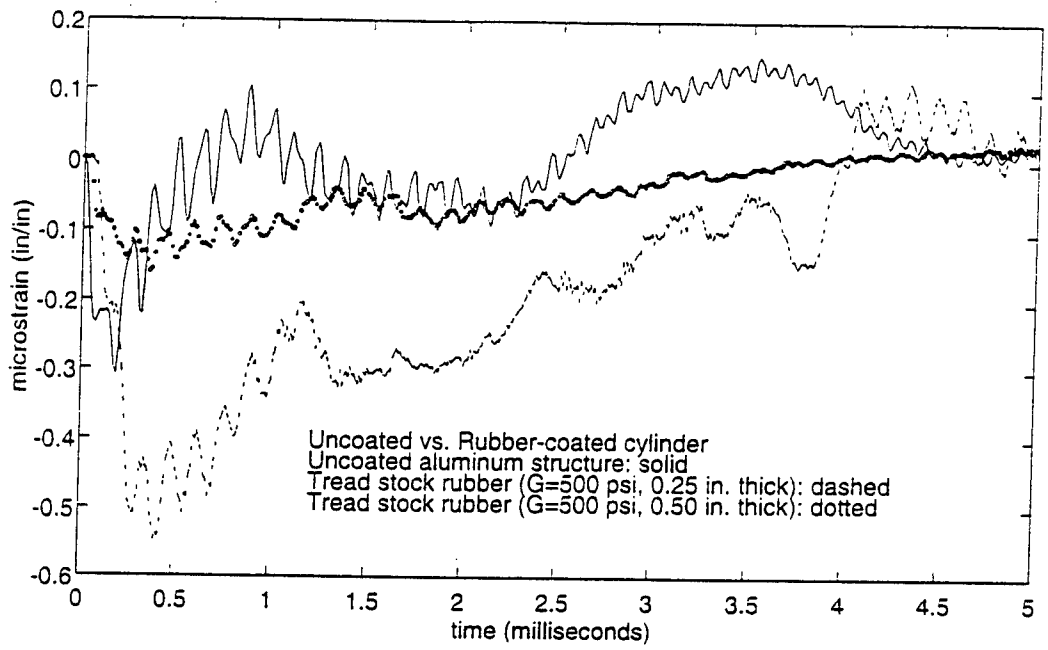

Figure 66. Hoop strain at position C for uncoated vs. coated aluminum cylinders of varying coating thicknesses and constant shear modulus of 500 psi

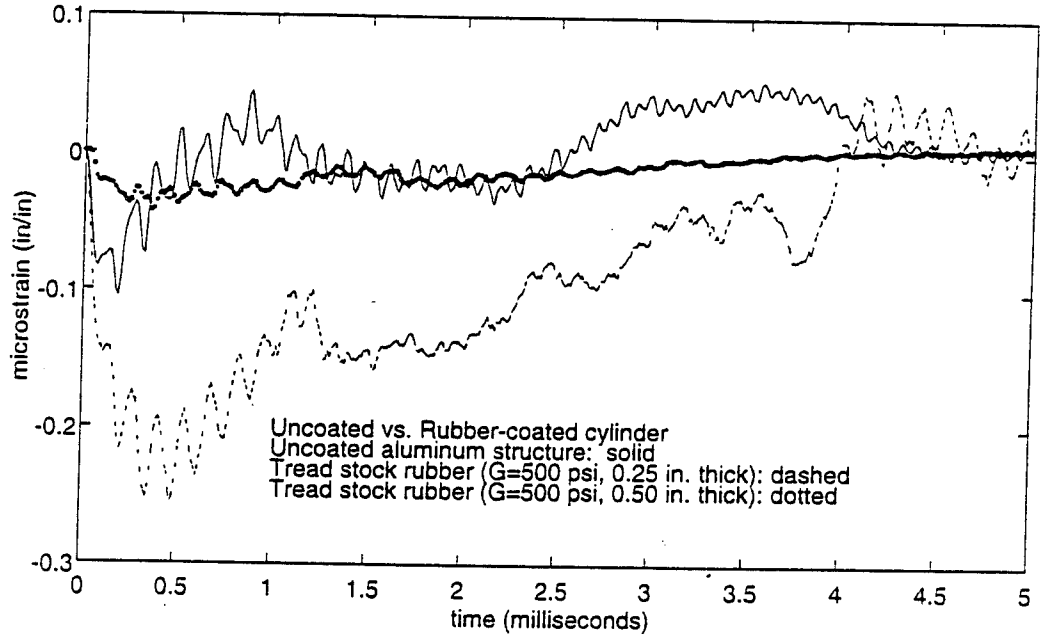

Figure 67. Axial strain at position C for uncoated vs. coated aluminum cylinders of varying coating thicknesses and constant shear modulus of 500 psi

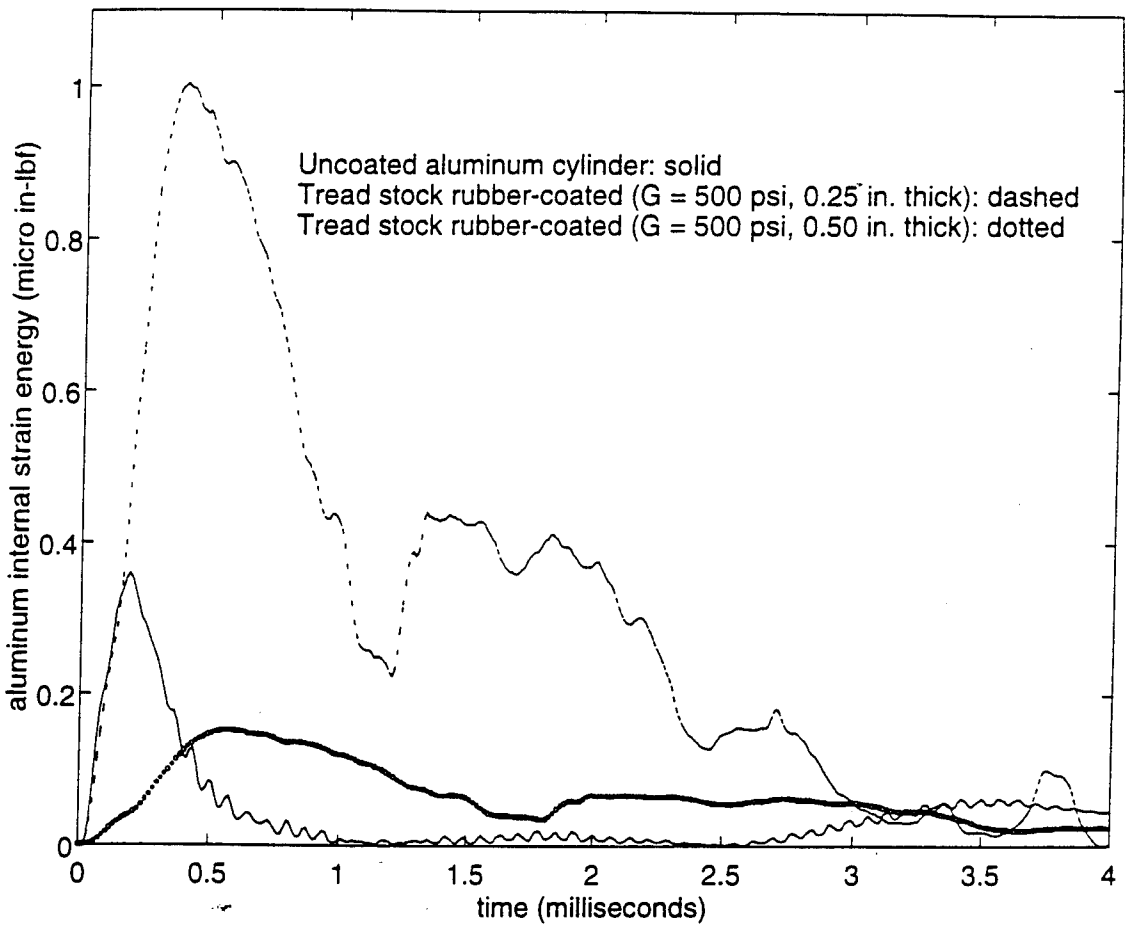

Figure 68. Internal energy of aluminum shell for uncoated vs. coated cylinders of varying thicknesses and constant shear modulus of 500 psi

VI. CONCLUSIONS

This parametric study analyzes the dynamic response of a one- and two-dimensional, coated structures subjected to a unit step pressure wave. The free end of the one-dimensional system is bounded by either air or water. The two-dimensional infinite cylinder is externally bounded by water.

The air-bounded, one-dimensional system response is characterized by alternating compression and release of the structure regardless of the nature of the coating material. This cyclical response is repeated throughout the duration of the external loading. The elastic coating with reduced impedance induces a higher stress magnitude in the underlying aluminum structure. Fluctuation of the stress wave is manifested as a series of compressive and tensile waves between the initial compression wave and the final relieving wave as a result of interaction at the interface and system boundaries. The period between successive zero-stress states increases with decreasing elastic coating impedance leaving the structure in a higher net compressive stress state for a longer duration of time. The nearly incompressible rubber coating induces a series of complex compressive and tensile waves in the structure. In general, a decreasing rubber shear modulus caused an increasing stress magnitude in the structure.

The release of a portion of the stress wave energy is evident in the water-bounded, one-dimensional system. For an elastic coating, the stress response is identical to that of the air-bounded system in its shape and periodicity only the water acts to dampen the stress energy. This damping results in reduced magnitudes in successive stress wave peaks as a function of time. The same phenomenon is observed in the one-dimensional systems having nearly incompressible rubber coatings. The nodal velocity of the aluminum structure increases with a decreasing rubber shear modulus. The softer

rubber coating alters the magnitude of the compressive wave. A softer rubber coating concentrates the stress wave within the structure, which contributes to increased stress magnitudes. This study warrants further investigation into structures coated with a nearly incompressible rubber material.

The results of this study show that a threshold value for a shear modulus and a coating thickness exists for a rubber coated model. A more favorable dynamic response accompanies a shear modulus above this value, while an adverse effect results below this value. A rubber shear modulus above 6000 psi for the one-dimensional system regardless of the bounding medium and above 500 psi for the infinite cylinder ensures a more favorable response for the present structure. The threshold value may vary depending upon the geometry and material properties of both the coating and the structure. It may also be given in terms of a critical difference. The critical difference is the difference in the impedances, ρc_o, between the rubber coating at the threshold value and the elastic structure.

LIST OF REFERENCES

1. Nelson, K.W., Shin, Y.S., Kwon, Y.W., "Failure of Aluminum Cylinder from Underwater Shock Effects," *63rd Shock and Vibration Symposium*, Las Cruces, NM, October 1992, pp. 83 - 95.

2. Fox, P.K., Kwon, Y.W., Shin, Y.S.,*Nonlinear Response of Cylindrical Shells to Underwater Explosion: Testing and Numerical Prediction Using VEC/DYNA3D*, Report NPS-ME-92-002, Naval Postgraduate School, Monterey, CA, March 1992.

3. Chisum, J.E., *Response Predictions for Double Hull Cylinders Subjected to Underwater Shock Loading*, Master's Thesis, Naval Postgraduate School, Monterey, CA, 1992.

4. Kwon, Y.W., Bergersen, J.K., Shin, Y.S., "Effect of Surface Coatings on Cylinders Subjected to Underwater Shock," *Shock and Vibration*, Vol. 1, No. 3, pp. 253 - 265, 1994.

5. Livermore Software Technology Corporation Report 1018, *VEC/DYNA3D User's Manual (Nonlinear Dynamic Response of Structure in Three Dimensions*, by D.W. Stillman and J.O. Hallquist, June 1990.

6. Livermore Software Technology Corporation Report 1019, *LS-INGRID: A Pre-processor and Three-Dimensional Mesh Generator for the Programs LS-DYNA3D, LS-NIKE3D, and TOPAZ-3D, Version 3.0*, by D.W. Stillman and J.O. Hallquist, June 1991.

7. Livermore Software Technology Corporation Report 1009, *LS-TAURUS: An Interactive Post-Processor for the Programs LS-DYNA3D, LS-NIKE3D, and TOPAZ-3D*, by J.O. Hallquist, April 1990.

8. DeRuntz, J.A. Jr., "The Underwater Shock Analysis Code and its Applications," Paper presented at the 60th Shock and Vibration Symposium, Virginia Beach, VA, 1989.

9. Geers, T.L., "Residual Potential and Approximate Methods for Three-Dimensional Fluid-Structure Interaction Problem," *Journal of the Acoustic Society of America*, Vol. 49, pp. 1505 - 1510, 1971.

10. Mooney, M., "A Theory of Large Elastic Deformation," *Journal of Applied Physics*, Vol. 11, pp. 582 - 592, 1940.

11. Kolsky, H., *Stress Waves in Solids*, New York, Dover Publications, Inc., 1963.

INITIAL DISTRIBUTION LIST

		No. copies
1.	Defense Technical Information Center Cameron Station Alexandria, VA 22304-6145	2
2.	Library, Code 052 Naval Postgraduate School Monterey, CA 93943-5101	2
3.	Professor Y.S. Shin, Code ME/Sg Department of Mechanical Engineering Naval Postgraduate School Monterey, CA 93943	2
4.	Professor Y.W. Kwon, Code ME/Kw Department of Mechanical Engineering Naval Postgraduate School Monterey, CA 93943	2
5.	Naval Engineering Curricular Office, Code 34 Naval Postgraduate School Monterey, CA 93943-5000	1
6.	Dr. Kent Goering Defense Nuclear Agency 6801 Telegraph Road Alexandria, VA 22310	1
7.	Mr. Douglas Bruder Defense Nuclear Agency 6801 Telegraph Road Alexandria, VA 22310	1
8.	Mr. Erik A. Rasmussen Code 1720.4 Naval Surface Warfare Center Carderock Division Bethesda, MD 20084-5000	1
9.	Dr. Roshdy S. Barsoum Office of Naval Research Mechanics Division, Code 1132 800 North Quincy Street Arlington, VA 22217-5000	1
10.	LT Thomas P. Brasek, USN 15372 Wetherburn Ct. Centreville, VA 22020	1